Geballe Laboratory for Advanced Materials
McCullough Building
Stanford University
Stanford CA 94305

Final Technical Report

Report for the Period

4/1/97-9/30/00

on

PREPARATION AND EVALUATION OF PHOSPHIDE SKUTTERUDITES

ONR Grant # N00014-97-1-0524-P00002

Submitted to

Office of Naval Research
Program Officier John C. Pazik, ONR 331
Ballston Centre Tower One
800 North Quincy Street
Arlington, VA 22217-5660

PI: Robert S. Feigelson

Submitted by
The Board of Trustees of
The Leland Stanford Jr. University
Stanford, California 94305

20010124 164

REPORT DOCUMENTATION PAGE

Public reporting burden for this collection of information is estimated to average 1 hour per response, including the time for reviewing instructions, searching data sources, gathering and maintaining the data needed, and completing and reviewing the collection of information. Send comments regarding this burden estimate or any other aspect of this collection of information, including suggestions for reducing this burden to Washington Headquarters Service, Directorate for Information Operations and Reports, 1215 Jefferson Davis Highway, Suite 1204, Arlington, VA 22202-4302, and to the Office of Management and Budget, Paperwork Reduction Project (0704-0188) Washington, DC 20503.
PLEASE DO NOT RETURN YOUR FORM TO THE ABOVE ADDRESS.

1. REPORT DATE *(DD-MM-YYYY)*	2. REPORT TYPE	3. DATES COVERED *(From - To)*
16-01-2001	Final Technical Report	April 1997 - September 2000

4. TITLE AND SUBTITLE

Preparation and Evaluation of Phosphide Skutterudites

5a. CONTRACT NUMBER

5b. GRANT NUMBER
N00014-97-1-0524-P00002

5c. PROGRAM ELEMENT NUMBER

6. AUTHOR(S)

Feigelson, Robert S. (Principal Investigator)

Watcharapasorn, Anucha

DeMattei, Robert C.

5d. PROJECT NUMBER

5e. TASK NUMBER

5f. WORK UNIT NUMBER

7. PERFORMING ORGANIZATION NAME(S) AND ADDRESS(ES)

Geballe Laboratory for Advanced Materials

Stanford University

Stanford, CA 94305

8. PERFORMING ORGANIZATION REPORT NUMBER

CMR P-96-12(N)

SPO 17633

9. SPONSORING/MONITORING AGENCY NAME(S) AND ADDRESS(ES)

Office of Naval Research, ONR 331

800 North Quincy Street

Arlington, VA 22217-5660

10. SPONSOR/MONITOR'S ACRONYM(S)

ONR

11. SPONSORING/MONITORING AGENCY REPORT NUMBER
FTR

12. DISTRIBUTION AVAILABILITY STATEMENT

Approved for public release; distribution unlimited.

13. SUPPLEMENTARY NOTES
The view, opinions and/or findings contained in this report are those of the author(s) and should not be construed as an official Office of Naval Research position, policy, or decision, unless so designated by other documentation.

14. ABSTRACT
This report summarizes a three and a half year program on the synthesis of phosphide skutterudite compounds using direct reaction and flux methods as well as a newly developed technique, the molten salt electrodeposition. A number of successfully prepared materials were measured for their thermoelectric properties as a function of temperature. It was found that some of these phosphide compounds exhibited semiconducting behavior in contrast to their antimonide analogs. This provided an opportunity to investigate skutterudite compounds having electrical properties ranging from semiconductors to semimetals/metals when phosphorus was replaced by antimony. In addition, the effect of anion size and mass on thermal conductivity of these compounds were experimentally verified. By extending our study to a binary cobalt phosphide-arsenide solid solution, we found that the thermoelectric properties were improved. We expected that this result could be applied to other filled ternary compounds, including the state-of-the-art $CeFe_4Sb_{12}$.

15. SUBJECT TERMS

Phosphide compounds, Skutterudites, Thermoelectric Materials, High-Temperature Synthesis, Transport Properties

16. SECURITY CLASSIFICATION OF:			17. LIMITATION OF ABSTRACT	18. NUMBER OF PAGES	19a. NAME OF RESPONSIBLE PERSON
a. REPORT	b. ABSTRACT	c. THIS PAGE	UL	64	Anucha Watcharapasorn
unclassified	unclassified	unclassified			19b. TELEPONE NUMBER *(Include area code)* 650-723-4874

Standard Form 298 (Rev. 8-98)
Prescribed by ANSI-Std Z39-18

TABLE OF CONTENTS

Abstract

This research project, which was a close collaboration between Stanford University and the Jet Propulsion Laboratory, focused on the synthesis and characterization of phosphide based skutterudite compounds such as CoP_3, $CeFe_4P_{12}$, $CeRu_4P_{12}$, $CoP_{3-x}As_x$, etc. Direct synthesis and recrystallization from a Sn flux were the two main techniques employed in our experiments. In addition, electrochemical synthesis techniques for the preparation of some cobalt binary skutterudite compounds have been developed and successfully used for the first time at Stanford University.

Thermoelectric measurements were carried out on the synthesized materials and the data used to deduce crucial information on the transport properties of these compounds. A number of phosphide skutterudites show semiconducting behavior in contrast to their antimonide analogs which normally are metallic or semimetallic. The effects of void filling and lattice disorder on the reduction of the thermal conductivity was also observed in the phosphide compounds, in agreement with those found for the antimonides.

The results from binary phosphide-arsenide solid solutions showed an unexpected enhancement in the Seebeck coefficient which led to higher thermoelectric figures of merit compared with related binary compounds. This indicates that it should be possible to improve the thermoelectric properties of the many of the skutterudite materials, including the most promising $CeFe_4Sb_{12}$.

I. Introduction

Materials which can achieve very high thermoelectric energy conversion efficiency (ZT) at low cost are desirable for a number of military and consumer applications, in particular cooling and power generation applications.

A JPL coordinated effort to search for new more efficient thermoelectric materials was initiated about three years ago under ONR and DARPA support. A large part of this program had to do with the skutterudite family of compounds, some of which were found by JPL to have exceptional thermoelectric properties. Team members in this program included the Naval Research Laboratory (NRL), Stanford University (SU), Rensselaer Polytechnic Institute (RPI) and Westinghouse Electric Corporation (WEC). The overall goal of the program was to demonstrate that novel materials with ZT values greater than 3.0 could be obtained. Stanford's role in this program, which was begun in April 1997, was to study the phosphide-based skutterudites. This two and a half year study, in parallel with a large research effort on the antimonide-based skutterudites, was designed to provide a better understanding of the transport properties in the skutterudites in general.

At the beginning of this project, a thorough search of phosphide synthesis techniques in general was undertaken, including methods previously used for the preparation of samples of the binary and ternary phosphide skutterudites and solid solutions. Two of these techniques, the direct synthesis from pure elements and/or compounds and recrystallization from a Sn flux method, were selected. Each of the two techniques have their advantages and disadvantages which are discussed in the experimental section.

Samples prepared were characterized by a number of analytical methods to determine their chemical, crystallographic, microstructural and thermodynamic properties. The thermoelectric property results were compared with those obtained for the more common antimonide skutterudites. The most promising of the phosphide skutterudite materials produced were analyzed more extensively, and suggestions for improving their thermoelectric properties provided in this report. Near the end of this project, the scope of this study was extended to include arsenide

4

skutterudites and their solid solutions with phosphides. Some of these materials were expected to be semiconductors with higher bond strength than the antimonides, thereby rendering these compounds attractive for high temperature applications. This report summarizes the experimental results as well as indicates any essential information regarding the synthesis and analysis of phosphide based skutterudite compounds.

II. Background

A. Thermoelectricity and Thermoelectric Materials

In 1821, Seebeck [1] produced the first thermoelectric effect where a current was generated from a closed loop of two dissimilar conductors when one of the junction was heated. Peltier [2], on the other hand, observed that, when an electric current was passed through such loop, heat was either absorbed or generated depending on the direction of the current. However, the theoretical treatment of these phenomena were not developed until Kelvin [3], in 1851, related these two phenomena using the concept of thermodynamics. His treatment later led to a calculation of thermoelectric conversion efficiency both for power generation and refrigeration. In Figure 1, a schematic drawing of a simple thermoelectric power generator and refrigerator are shown.
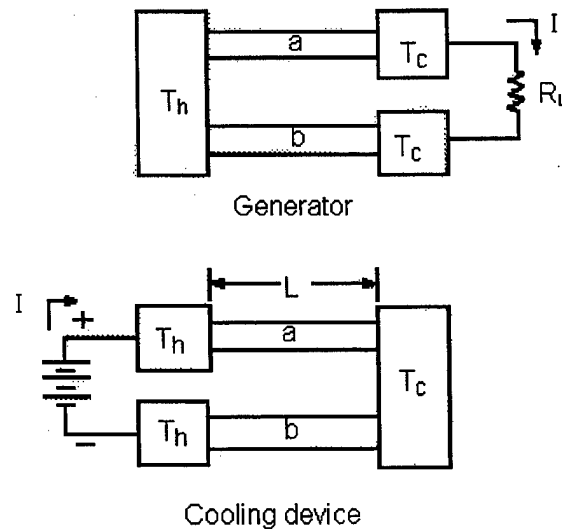

Figure 1. Schematic drawing of a Seebeck-effect thermoelectric generator and a Peltier-effect thermoelectric cooling device. The elements marked Th and Tc are heat reservoirs and are assumed to have zero electrical resistance. The elements marked a and b are called arms. To maximize the efficiency of the device, the one marked *a* usually has a positive   absolute Seebeck coefficient, while the one marked *b* usually has a negative coefficient. [4]

In the case of power generation, it was shown [5] that the generating efficiency is expressed as:

$$\eta = \frac{I^2 R_L}{\alpha_{ab} T_h I - \frac{1}{2} I^2 R + K \Delta T} \tag{1}$$

$$I = \frac{\alpha_{ab} \Delta T}{R + R_L} \tag{2}$$

where R_L = load resistance, α = Seebeck coefficient of the couple, Th = temperature at the hot junction, Tc = temperature at the cold junction, ΔT = Th - Tc, R = total resistance from thermoelectric arms, and K = total thermal conductance of thermoelectric arms. The nominator in Eqn. (1) is the energy supplied to the load and the denominator corresponds to the heat energy absorbed at the hot junction. Using Eqn. (1) and (2) and assuming that both arms have equal length and element a has unit cross-sectional area, the maximum efficiency with respect to the load resistance and shape factor of the arms can be expressed as

$$\eta_{max} = \left(\frac{\Delta T}{T_h} \right) \left[\frac{(1 + Z_{ab} \overline{T})^{1/2} - 1}{(1 + Z_{ab} \overline{T})^{1/2} + (T_c / T_h)} \right] \tag{3}$$

$$Z_{ab} = \frac{\alpha_{ab}^{\,2}}{[(\rho_a \kappa_a)^{1/2} + (\rho_b \kappa_b)^{1/2}]^2} \tag{4}$$

where $\overline{T} = (T_h + T_c) / 2$ and Z_{ab} is called the figure of merit of the couple. The figure of merit for single material can be expressed as

$$Z = \frac{\alpha^2}{\rho \kappa} = \frac{\alpha^2 \sigma}{\kappa} \tag{5}$$

where ρ is the electrical resistivity ($=1/\sigma$), σ is the electrical conductivity, α is the Seebeck coefficient and κ is the thermal conductivity. The mathematical treatment of thermoelectric cooling devices is similar and it was shown that $Z\overline{T}$ again plays an important role in determining the conversion efficiency [5].

It is clear that the efficiency of a thermoelectric power generation device is limited by the Carnot efficiency ($\Delta T/T_h$) and a material parameter (Z). Figure 2 is the plot of the maximum

efficiency of a material as a function of $Z\overline{T}$ and the ratio of the temperature at the cold and hot junctions. This plot shows two significant aspects of the possibility of manufacturing thermoelectric devices. First, it shows that $Z\overline{T}$ value of at least 3.0 (for Tc/Th = 0.3) is required for new materials in order to be competitive with other energy conversion devices, for examples, solar cells which currently have maximum conversion efficiency of around 30% and steam turbines whose efficiency is higher than 35%. Second, it shows that the efficiency increases with increasing temperature at the hot junction which means that a suitable thermoelectric material should be stable at such high temperatures. This latter point is discussed further in the section dealing with the properties of various thermoelectric materials.
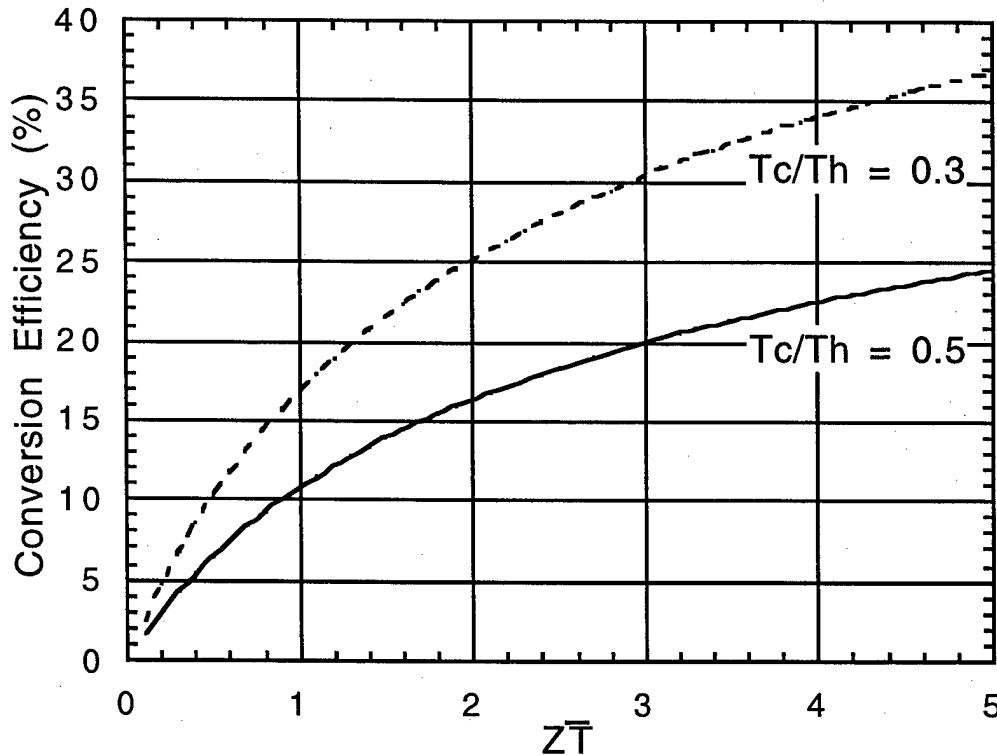

Figure 2. A plot of conversion efficiency of a thermoelectric material as a function of the figure of merit and temperatures at the junctions.

A large number of materials have been studied for their possible use in thermoelectric applications. In metals and metal alloys, optimization of an individual property is limited by the

Wiedemann-Franz-Lorenz law which states that the ratio of thermal conductivity to electrical conductivity is a constant with respect to temperature. This relationship is shown in Eqn. (6),

$$\kappa_e = \gamma(k/e)^2 \sigma T \qquad (6)$$

where κ_e is the electronic thermal conductivity, $\gamma = \pi^2/3$, k is the Boltzmann constant, e is the electronic charge, σ is the electrical conductivity, and T is the absolute temperature. In addition, the Seebeck coefficients of most metals are only 10 $\mu V/K$ or less, thus providing efficiency of less than 1 percent [6] which is considered uneconomical for power generation.

Later, it was found that large Seebeck coefficients in excess of 100 $\mu V/K$ could be achieved in some semiconducting materials. However, in semiconductors, the ratio of electrical to thermal conductivity is lower than that of metals and the need to improve this ratio is apparent. In 1956, Ioffe and his co-workers [7] demonstrated that the ratio σ/κ ($\kappa = \kappa_e + \kappa_{lattice}$) could be increased by alloying the material with isomorphous elements or compounds. In this case, the additional disorder in the lattice is introduced to scatter thermal energy carrying phonons. Table 1 lists a number of state-of-the-art thermoelectric materials along with their maximum $Z\overline{T}$ values and corresponding temperatures at which these values are attained.

Table 1. A list of thermoelectric materials and their maximum figure of merits.

Compound (p-type)	$Z\overline{T}$	Temperature (K)
Bi_2Te_3	1.0	300
TAGS (Te-Ag-Ge-Sb)*	1.2	700
PbTe	0.85	750
SiGe	0.6	1100
Zn_4Sb_3	1.4	673
$CeFe_4Sb_{12}$	1.4	873

* This compound has phase instability.

These compounds were characterized as highly doped semiconductors or semimetals which agree well with the prediction from theoretical treatment of Ioffe [8]. Nevertheless, these materials need to be optimized in order to improve their thermoelectric efficiency. In this report, the discussion will be focused mainly on a class of materials called "skutterudites" which includes $CeFe_4Sb_{12}$ as one of the compounds.

B. Skutterudite Compounds

Simple binary skutterudite compounds (naturally occurring $CoAs_3$ is the prototype) are formed with all nine possible combinations of the elements Co, Rh, Ir with P, As, Sb. In this structure each metal atom has six bonds to a pnicogen, forming distorted octahedra, and each of the three pnicogens has two bonds to another pnicogen and two bonds to a metal atom, as shown in Figure 3 [12]. The unit cell of the skutterudite structure (cubic, space group *Im3*) contains square radicals $[As_4]^{4-}$. This anion, located in the center of the smaller cube, is surrounded by 8 Co^{3+} cations. The unit cell consists of the 8 smaller cubes (octants) described above, but two of them do not contain anions ($[As_4]^{4-}$) in the center, hence the term "unfilled" is sometimes used to indicate skutterudite materials that contain empty octants. This atomic arrangement is necessary to keep the ratio $Co^{3+}:[As_4]^{4-} = 4:3$. Thus, the typical coordination structure is $Co_8[As_4]_6 = 2Co_4[As_4]_3$ containing 32 atoms per cell.
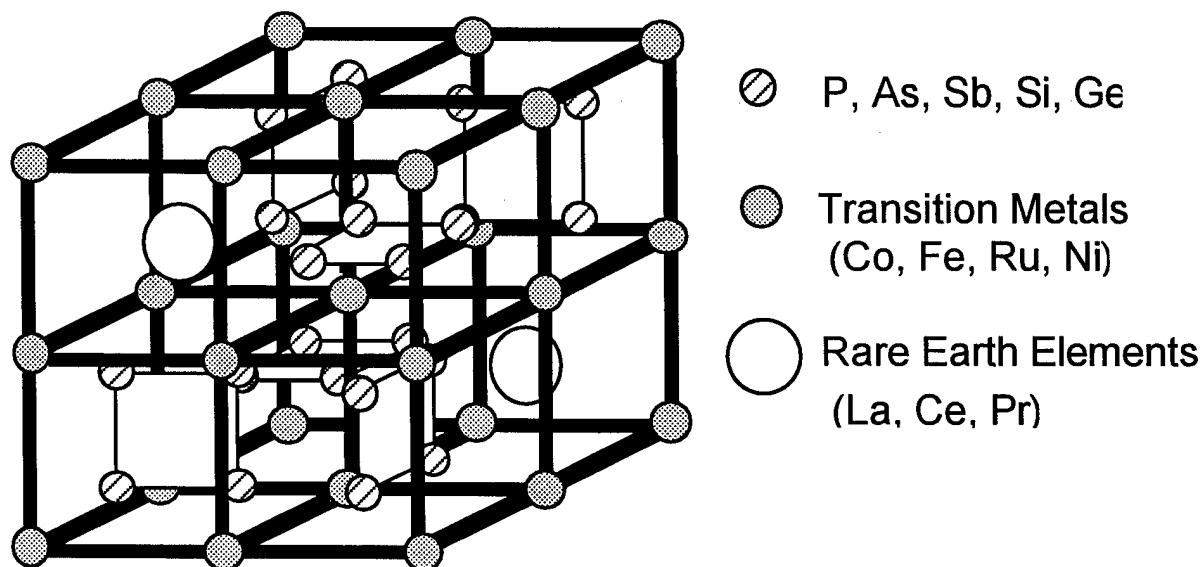
Figure 3. Illustration of the skutterudite structure. The structure is called "filled" when the two empty octants in the unit cell are filled with a rare-earth or alkaline earth atom.

A number of unfilled solid solutions can be prepared by substituting atoms either at the metal and/or pnicogen sites. Furthermore, "filled" ternary compounds result when empty octants (see Figure 3) are filled with atoms, usually rare-earth elements, for example, $CeFe_4Sb_{12}$. Therefore, it can be seen that the number of possible combinations of elements needed to form the skutterudite structure is very large. This is considered one of the advantages over other currently used thermoelectric materials where the number of isostructural materials is quite limited. Figure 4 summarizes the elements that have been used to prepare skutterudite materials.

PERIODIC CHART OF THE ELEMENTS

IA	IIA	IIIB	IVB	VB	VIB	VIIB	VIII			IB	IIB	IIIA	IVA	VA	VIA	VIIA	INERT GASES
1 H 1.00797																1 H 1.00797	2 He 4.0026
3 Li 6.939	4 Be 9.0122											5 B 10.811	6 C 12.0112	7 N 14.0067	8 O 15.9994	9 F 18.9984	10 Ne 20.183
11 Na 22.9898	12 Mg 24.312											13 Al 26.9815	14 Si 28.086	15 P 30.9738	16 S 32.064	17 Cl 35.453	18 Ar 39.948
19 K 39.102	20 Ca 40.08	21 Sc 44.956	22 Ti 47.90	23 V 50.942	24 Cr 51.996	25 Mn 54.9380	26 Fe 55.847	27 Co 58.9332	28 Ni 58.71	29 Cu 63.54	30 Zn 65.37	31 Ga 69.72	32 Ge 72.59	33 As 74.9216	34 Se 78.96	35 Br 79.909	36 Kr 83.80
37 Rb 85.47	38 Sr 87.62	39 Y 88.905	40 Zr 91.22	41 Nb 92.906	42 Mo 95.94	43 Tc (99)	44 Ru 101.07	45 Rh 102.905	46 Pd 106.4	47 Ag 107.870	48 Cd 112.40	49 In 114.82	50 Sn 118.69	51 Sb 121.75	52 Te 127.60	53 I 126.904	54 Xe 131.30
55 Cs 132.905	56 Ba 137.34	*57 La 138.91	72 Hf 178.49	73 Ta 180.948	74 W 183.85	75 Re 186.2	76 Os 190.2	77 Ir 192.2	78 Pt 195.09	79 Au 196.967	80 Hg 200.59	81 Tl 204.37	82 Pb 207.19	83 Bi 208.980	84 Po (210)	85 At (210)	86 Rn (222)
87 Fr (223)	88 Ra (226)	‡89 Ac (227)	104 Rf (261)	105 Db (262)	106 Sg (266)	107 Bh (262)	108 Hs (265)	109 Mt (266)	110 ? (271)	111 ? (272)	112 ? (277)						

Numbers in parenthesis are mass numbers of most stable or most common isotope.

Atomic weights corrected to conform to the 1963 values of the Commission on Atomic Weights.

The group designations used here are the former Chemical Abstract Service numbers.

*Lanthanide Series

58 Ce 140.12	59 Pr 140.907	60 Nd 144.24	61 Pm (147)	62 Sm 150.35	63 Eu 151.96	64 Gd 157.25	65 Tb 158.924	66 Dy 162.50	67 Ho 164.930	68 Er 167.26	69 Tm 168.934	70 Yb 173.04	71 Lu 174.97

‡Actinide Series

90 Th 232.038	91 Pa (231)	92 U 238.03	93 Np (237)	94 Pu (242)	95 Am (243)	96 Cm (247)	97 Bk (247)	98 Cf (249)	99 Es (254)	100 Fm (253)	101 Md (256)	102 No (256)	103 Lr (257)

Figure 4. A periodic table showing many possible combinations of elements in skutterudite materials: ▨ corresponds to filling atoms, ◹ transition metal atoms, and ▦ anion atoms.

Because a large number of skutterudite materials exist, a wide range of electrical and thermal properties are expected. This is very useful when one tries to optimize the thermoelectric properties by changing the compositions of a compound. Theoretical treatment has shown that the electrical properties are optimized in materials that have high carrier mobilities with relatively large band mass [5]. Another factor which also plays an important role is the carrier concentration which Ioffe [8] has shown should be on the order of 10^{19} cm^{-3}. High carrier mobilities are usually found associated with crystal structures having a high degree of covalency. It has been shown that the bonding is predominantly covalent in the skutterudite structure and high hole mobility values have been measured on several skutterudite compounds including: $IrSb_3$, $RhSb_3$, $CoSb_3$, $CoAs_3$, $RhAs_3$ and RhP_3 [13].

Unfortunately, the room temperature thermal conductivity of binary skutterudites (100-150 mW/cmK) was found to be too high to produce high ZT values. Substantial reductions in the lattice thermal conductivity must be obtained to achieve values comparable to those of state-of-the-art thermoelectric materials such as Bi_2Te_3-alloys (15-20 mW/cmK), PbTe-alloys (10-20 mW/cmK) and Si-Ge alloys (40-50 mW/cmK). The contribution of the crystal lattice, through phonon heat conduction, to the total thermal conductivity can be reduced by more effectively scattering phonons. Several approaches have been used to reduce the lattice thermal conductivity of these materials. Experimental efforts have successfully demonstrated that low thermal conductivity values could be achieved in heavily doped n-type binary compounds, solid solutions, ternary compounds, and also filled skutterudites. In these materials, the lattice contribution to the thermal conductivity is greatly reduced, with room temperature values ranging from 15 to 30 mW/cmK. Various scattering mechanisms are responsible for the reductions in lattice thermal conductivity including: electron-phonon scattering in heavily doped samples, mass and strain fluctuation scattering in solid solutions and alloys, electron charge transfer scattering in mixed-valence ternary compounds, and void filler scattering in filled skutterudite compounds [22].

The electrical properties of the ternary skutterudites can vary substantially from the results obtained on the binary compounds. They range from very heavily doped ($Ru_{0.5}Pd_{0.5}Sb_3$) to more lightly doped ($RuSb_2Te$), and from extrinsic p-type behavior ($FeSb_2Te$) to mixed conduction n-type behavior ($Fe_{0.5}Ni_{0.5}Sb_3$). These findings indicate that significant changes in band structure and doping behavior were caused by changes in the atomic and electronic structure. In particular, fluctuations in the valence of the transition metal atoms could be imposed by the need to conserve the skutterudite crystal structure. Understanding and controlling these charges is a key step in designing a skutterudite composition with superior thermoelectric properties. The study of the existence and transport properties of ternary skutterudite phosphides is undoubtedly critical to these efforts.

A large number of materials with a filled skutterudite crystal structure have already been synthesized (see [15-19]). The composition of these types of compounds can be represented by the

formula LnT_4Pn_{12} (Ln=La, Ce, Pr, Nd, Sm, Eu, Gd, Th and U; T= Fe, Ru, Os; Pn=P, As, Sb). Most of these compounds behave as metals, or very heavily doped p-type semimetals. Some of these compositions, based on $CeFe_4Sb_{12}$, have been recently prepared by a combination of melting and powder metallurgy techniques and have shown exceptional thermoelectric properties in the 350-700 °C temperature range [11]. At room temperature, $CeFe_4Sb_{12}$ behaves as a p-type semimetal, but with a low thermal conductivity and surprisingly large Seebeck coefficient. These results are consistent with some recent band structure calculations on these compounds [20]. Replacing Fe with Co in $CeFe_4Sb_{12}$ and increasing the Co:Fe atomic ratio resulted in an increase in the Seebeck coefficient values. Measurements on bulk samples with a $CeFe_{3.5}Co_{0.5}Sb_{12}$ atomic composition and p-type conductivity resulted in dimensionless figure of merit ZT values of 1.5 at 600 °C [11]. While most of these compounds are metallic, it has been shown or predicted that some of them such as UFe_4P_{12}, $CeFe_4P_{12}$, $CeRu_4P_{12}$ and $CeFe_4As_{12}$ are semiconductors [15, 20, 21]. Thus, the study of some of the filled skutterudite phosphides is of great interest because it would allow a transition from a metallic to semiconducting behavior (opening of the band gap when substituting As and/or P for Sb in $CeFe_4Sb_{12}$). Since mixed conduction can be avoided at high temperatures in the materials with larger band gaps, this could lead to improved properties of these materials for power generation applications.

C. Synthesis Techniques for Phosphide Based Skutterudites

The synthesis and growth of compounds containing phosphorous is complicated and challenging because many of these materials are incongruently melting and/or have high vapor pressures (higher than arsenides and antimonides) and tend to dissociate at the elevated temperatures required for chemical reaction or melting to take place. Four techniques have been used in the past for synthesis of phosphide skutterudite compounds and are briefly described below.

14

a) Direct reaction of pure elemental mixtures

This technique was first described by Biltz and Heimbrecht [25] who synthesized the binary phosphide skutterudite, CoP_3, by heating a mixture of cobalt and phosphorus in sealed silica tubes. Based on this method, Rundqvist and Larsson also prepared this compound and briefly reported that CoP_3 has the $CoAs_3$-type structure with the cell dimension a = 7.706 ± 0.004 Å [26]. Later, Rundqvist and Ersson [27] concluded that completely reacted CoP_3 (without any unreacted phosphorus remaining) could be prepared by heating stoichiometric mixtures of cobalt and phosphorus in evacuated and sealed silica tubes at 950 - 1000 °C for some days, followed by sufficiently slow cooling of the tubes to room temperature. If the cooling of the CoP_3 was too rapid, some unreacted phosphorus was observed and x-ray diffraction showed weak CoP lines in addition to those of CoP_3. When a slight excess amount of phosphorus was used to make CoP_3, some unreacted phosphorus always remained in the system even after very long and careful heat treatment. The lattice constant measured at 22 °C was 7.7073 ± 0.0002 Å. Other binary phosphides (NiP_3, IrP_3, RhP_3, and PdP_3) and binary cobalt phosphide-arsenide solid solutions have also been synthesized using similar procedures [27-31].

It is worth noting that the binary skutterudite FeP_3 has not been synthesized experimentally. This may be due to the nature of the electronic structure in the skutterudite lattice. The most useful approach used to develop qualitative understanding of the bonding of covalent compounds is that of the molecular orbital theory. From the structure shown in Fig. 1, each of the phosphorus atoms contributes two electrons to two s bonds in the P_4 group, leaving three electrons for the metal - non metal bonds. Since each metal ion is surrounded by six non-metal ions in an octahedral coordination, there are six bonding and three non-bonding energy levels to be filled by available electrons [27]. In CoP_3, cobalt has nine valence electrons which, including the other nine electrons from six phosphorus atoms, are just enough to fill the available energy levels. For FeP_3, however, there is one less electron available to fill the non-bonding levels, hence causing the structure to be unstable. In NiP_3, there is one extra electron which can fill an antibonding level giving this material a metallic behavior [35].

15

The experimental procedure pioneered by Jeitschko and Braun [19] for synthesizing "filled" ternary phosphide skutterudites consisted of mixing stoichiometric amount of rare-earth metal filings, transition metals (Fe, Ru, or Os), and red P (sometimes in excess amount), and sealing them into evacuated silica tubes. These were rapidly heated to 1250 K and annealed for one week at 1050 K. X-ray diffraction patterns of the products frequently showed weak lines of binary phosphides in addition to those of the ternary compounds. Better results were obtained when the rare-earth metals were introduced into the mixture as monophosphides which can be easily ground into a fine powder.

b) Recrystallization from a Sn flux

This technique was first developed and used by Jolibois [32] who synthesized NiP_3 by heating a nickel-tin alloy with excess phosphorus and dissolving the tin phosphide formed in an HCl acid solution. Later, a number of binary phosphide skutterudites were also prepared using similar procedures [24,25, 32-34].

Single crystals of a "filled" ternary compound, $LaFe_4P_{12}$, was first grown by Jeitschko and Braun [19]. Starting materials were La filings, Fe powder, red P and Sn in the atomic ratio of 1:4:20:50. The mixture was sealed in evacuated silica tubes and annealed for one week at 777 °C. After slow cooling (2 °C/h), the samples were treated with moderately dilute HCl acid (1:1) to dissolve the Sn matrix. The resulting crystals of $LaFe_4P_{12}$ had truncated octahedral habit with diameters up to 0.2 mm. Analysis for residual Sn impurities of these crystals involved dissolving the crystals in a melt containing Na_2CO_3 and Na_2O_2 (in a ratio of 1:3). After cooling, the melt was dissolved in hydrochloric acid. Flame absorption analysis indicated a Sn content of 0.035%. The authors assumed that some of this was due to heterogeneous flux inclusions. By replacing La with other lanthanide elements, and Fe with Ru or Os, a series of ternary compounds could be prepared [17, 35, 37, 38]. Th and U from the actinide group have also been used as filling atoms in the skutterudite lattice. Ternary compounds crystallized from Sn fluxes were characterized for their crystal structures and other properties [35, 36, 39].

Another type of "filled" lanthanide compounds (based on a $-Co_4P_{12}$ instead of $-Fe_4P_{12}$ framework) was prepared by Zemni et al. [40]. The elements were in the atomic ratio of 1:4:12 with the tin content varying from between 80 and 85 wt%. The mixtures were sealed in silica tubes under vacuum and heated for 2 days at 1300 K, followed by slow cooling (3 °C/h) to 800 K and quenching in water. After treating the resulting mixtures electrochemically to remove the Sn matrix, crystals of $Tr_xCo_4P_{12}$ (Tr=La, Ce, Pr, Nd, Yb) were found. They had a cubic habit with dimensions up to 1 mm^3. Powder patterns were obtained using Si as an internal standard and the cell constants were refined by least-square calculations. The comparison of these parameters with that of CoP_3 gave the first indication of the incorporation of the rare earth in the skutterudite lattice. Their results were also confirmed by energy dispersive analysis using a scanning electron microscope which gave approximate composition: $Tr_{0.5}Co_4P_{12}$ for these phases without any inclusion of tin (detectability limit on the order of 1%). The structure refinement led to x=0.25 in $Ce_xCo_4P_{12}$ and x=0.2 in $La_xCo_4P_{12}$. The compositions for other ternary rare-earth cobalt phosphides were probably measured, but not published. They also reported that by changing the initial ratio Tr:Co:P in the tin melt, the same lattice parameters of the crystals were always obtained, which indicated a small homogeneity range for these compounds.

c) Chemical vapor deposition

CoP_3 single crystals of 80 mg weight and 3 x 3 x 1 mm^3 size were grown by this technique using chlorine as a transporting agent [41]. The authors reported that the crystals exhibited metallic reflection and had a cubic morphology. From their experimental procedure, the total time used to grow these crystals was approximately one month.

d) High pressure/high temperature synthesis

Munson and Kasper [42] prepared a skutterudite phase in the Co-P system under high pressure conditions. The material was obtained at 60 kbars and 1400 °C only when P/Co atomic ratio was in the vicinity of 4, and the chemical analysis gave the composition of $CoP_{3.90}$.

A number of phosphide skutterudites such as NiP_3 and other ternary compounds have also been prepared by high pressure/high temperature synthesis [21, 43, 44]. In these cases, a wedge-type cubic-anvil high pressure apparatus was used to produce dense polycrystalline samples. Normal procedure involved heating stoichiometric mixture of metals and phosphorus powders under pressures of 0.5 - 4 GPa and at temperatures between 1000 - 1200 °C.

III. EXPERIMENTAL PROCEDURES

During the course of this program, we used the direct reaction and recrystallization from a Sn flux methods to prepare a number of phosphorus-based skutterudite materials for property evaluation. A list of materials that were attempted is shown in Table 2 and 3. Successful experiments refer to the materials containing at least 95% skutterudite phase and their thermoelectric properties are reported in the next section. Moderately successful experiments include those that produced less than 95% of the skutterudite phase and therefore were not suitable for thermoelectric measurements. Unsuccessful experiments will refer to those that did not produce or produced only a small amount of the skutterudite phase.

It should be noted that a number of the material systems studied, especially for the flux systems, were complicated due to a lack of knowledge of their thermodynamic behavior, especially adequate phase diagrams. It was therefore quite difficult to find the optimum synthesis conditions for each system particularly when we were surveying a large number of different compounds. In addition, a number of the single phase materials produced were lost during re-processing and/or during the hot-pressing of samples for thermoelectric measurements. Although we tried to study the decomposition temperatures of some of these compounds by thermogravimetric analysis, the data were complicated by the reaction of phosphorus vapor with the platinum sample container used in these measurements. Nevertheless, the thermoelectric properties of a number of phosphide based compounds were measured and compared. Their data are discussed in the next section.

Table 2. A list of materials synthesized by the flux technique

Successful	CoP_3, $La_{0.24}Co_4P_{12}$, $CeFe_4P_{12}$, $CeRu_4P_{12}$, $PrFe_4P_{12}$
Moderately successful	$NiGeP_2$, $LaFe_4P_{12}$, $NdFe_4P_{12}$, $SmFe_4P_{12}$, $EuFe_4P_{12}$, $PrRu_4P_{12}$, $CeFe_4P_9As_3$
Unsuccessful	$CeCo_4Ge_3P_9$, $CeFe_4P_6As_6$, $LuFe_4P_{12}$, $TbFe_4P_{12}$, $YbFe_4P_{12}$

Table 3. A list of materials prepared by direct synthesis

Successful	CoP_3, $CoAs_3$, $CoSb_3$, $CoP_{0.75}As_{2.25}$, $CoP_{1.5}As_{1.5}$, $CoP_{2.25}As_{0.75}$, $La_xCo_4P_{12}$, $LaFe_4P_{12}$, $CeFe_4P_{12}$, $CeCo_4Si_{2.2}P_{9.8}$, $Ce_{0.16}Co_4Ge_{0.5}P_{11.5}$, $CeCo_4Si_3As_9$
Moderately successful	$NiGeP_2$, $Fe_{0.5}Ni_{0.5}P_3$, $CeFe_3CoP_{12}$, $CeFe_4As_{12}$, $LaCo_4Ge_3P_9$, $LaCo_4Si_3P_9$, $LaFe_3NiP_{12}$, $PrFe_2Co_2P_{12}$
Unsuccessful	$CoP_{3-x}Sb_x$, $CeFe_4P_{12-x}As_x$

In addition to the two experimental techniques mentioned, we also successfully developed a new technique for the preparation of skutterudite materials. Of this method, molten salt electrochemical synthesis was used to prepare cobalt phosphide, arsenide, and antimonide. The results of our experiments are discussed below, including some critical issues that need to be considered in order to successfully prepare these phosphide compounds. These include: (i) carrying out the synthesis under an inert or vacuum conditions, (ii) keeping the pressure of gaseous components inside a processing tube below the hoop strength of the fused quartz tube, (iii) controlling the heating/cooling rate.

A) Crystallization from a Sn flux

The main advantage of the flux technique over the direct reaction technique is that the phosphorus pressure at the reaction temperature can be reduced. In addition, reannealing experiments are not required and it provides the possibility of having physical measurements done on single crystals, provided that these crystals are large enough. In our experiments, the starting materials were elements of at least 99.9% purity. The molar ratio of the starting charge compositions for LnFe4P12 was Ln:Fe:P:Sn = 1:4:20:50 [19] (where Ln = a rare-earth metal) and for CoP_3, Co:P:Sn = 1:3:25. The mixture was loaded into 1.5 mm thick and 30 cm long fused silica tubes. The inside diameters of those tubes varied between 15 - 20 mm. After completing the preparation step, the tubes were quickly transferred to a vacuum station where they were evacuated until the pressure was less than 10^{-5} torr and then sealed. The mixture was heated in a resistance

furnace controlled by a programmable controller. The heating rate of 50 °C/h was normally used to allow for the dissolution of elemental components in the Sn melt and a rate of 2 °C/h was used in the cooling process. The soak temperatures were between 780 and 1000 °C and the soak time was about one week. The resultant materials were treated with an HCl acid solution in order to dissolve the Sn matrix and tin phosphide which formed during synthesis.

From our experiments, the method worked well for CoP_3, $CeFe_4P_{12}$ and $CeRu_4P_{12}$. The synthesized materials normally consisted of small shiny crystallites as well as black or gray powder as shown in Figure 5 (a) for CoP_3. The corresponding powder diffraction pattern is given in Figure 5 (b).

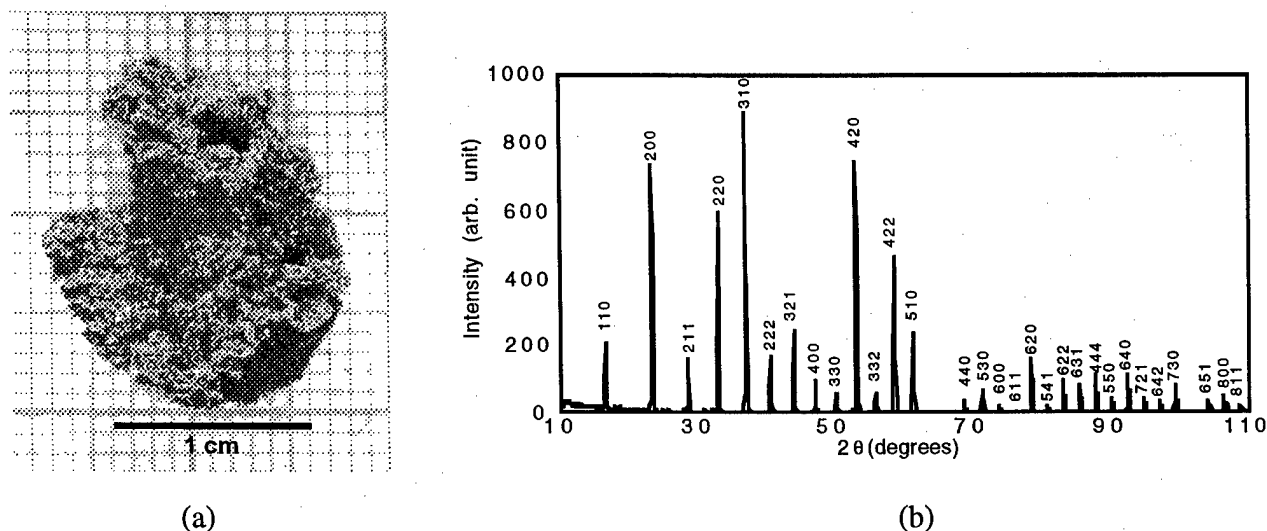(a)   (b)

Figure 5. (a) As synthesized CoP_3 from a Sn flux after HCl acid treatment. The agglomeration consisted of small crystallites and black powder which could be easily broken up and ground., (b) Powder X-ray diffraction pattern of CoP_3

In the case of $PrFe_4P_{12}$, a dense solid as well as a small amount of yellow particles was present in addition to small crystallites and black powder were present after synthesis when a soak temperature of 780 °C was used. X-ray analysis showed that the dense phase consisted mainly of two iron phosphides, FeP and FeP_2. The relative amount of skutterudite phase was about 30% as approximated from the diffraction pattern. An electron micrograph with qualitative energy dispersive x-ray analysis of the dense solid also confirmed the existence of iron phosphides as well

21

as a small amount of praseodymium phosphide, possibly PrP. Based on theoretical considerations of crystal growth from high-temperature solutions, there are a number of factors that may explain these results. These include 1) changes of the atmospheric conditions inside the sealed quartz tube, for example, the loss of phosphorus vapor pressure if the tube leaks, 2) too low a reaction or soak temperature for complete dissolution of the Pr metal into the tin melt, 3) reaction of the dissolved elemental components in the tin flux, and 4) impurities. This list is, by no mean, complete and other variables not mentioned here may also play a role in determining the crystallization behavior of the Sn solutions.

There was always a possibility that the processing tube was not completely sealed. In this case, P would react with oxygen in the atmosphere to form phosphorus pentoxide (P_2O_5). This would condense out on a cool surface in the form of a white powder. Since there was no sign of phosphorus vapor or P_2O_5 at or near the furnace, this did not seem to be a likely cause. Experiences from working with sealed silica tubes in many experiments also confirmed that leakage was not a problem.

An alternate assumption had to be made to determine the procedure for new experiments. The first assumption was that the soak temperature used was too low to allow homogenization of the melt. Increasing the temperature would mean higher mobility of atomic constituents and increased solubility of the solutes in the solution. Therefore the soak temperature of the next $PrFe_4P_{12}$ experiment was increased to 900 °C. The result was better than the previous run and the synthesized product was mainly the skutterudite phase. It consisted of tiny, shiny crystallites as well as a black powder as shown in Figure 6 (a).
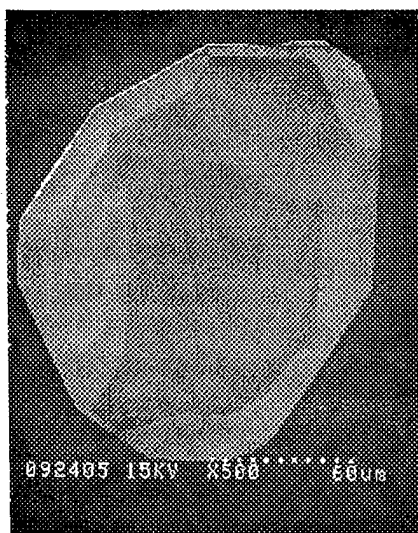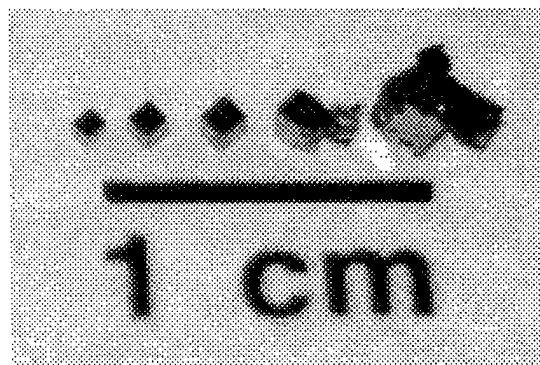
<center>(a)   (b)</center>

Figure 6. (a) A SEM picture of a single grain of $PrFe_4P_{12}$ grown from a Sn flux; (b) An optical photograph of $La_{0.24}Co_4P_{12}$ single crystals of various sizes.

We also studied the effect of void filling in a CoP_3 lattice by using La atoms. Following the procedure of Zemni et al. [40], crystals of up to 2 mm were obtained and they clearly exhibited the cubic morphology of the skutterudite structure (Figure 6 (b)). The electron microprobe analysis on these crystals gave an average composition of $La_{0.24}Co_4P_{12}$ which is in close agreement with previous findings from crystal structure refinement of this material [40]. The authors also found that varying the initial ratio of the melt components did not affect the value of its lattice parameter, which indicates a small homogeneity range for this compound. The inability to completely fill the -Co_4P_{12} framework with rare-earth atoms seems to be in agreement with that reported for rare-earth cobalt antimonides [45, 46]. It is possible that this concentration of La atoms may be the upper limit for stability of skutterudite structure.

A qualitative comparison of the crystallization behavior between -Fe_4P_{12} and -Co_4P_{12} systems was made. In figure 6 (a) and (b), the crystal sizes of the two compounds are quite different. The crystals of $La_{0.24}Co_4P_{12}$ were on the order of millimeters while those of $PrFe_4P_{12}$ were about ten times smaller as shown by the scales. This variation may be due to the higher solubility of La and Co in Sn, a smaller nucleation rate, and/or a larger crystallization range for

<center>23</center>

$La_{0.24}Co_4P_{12}$. Table 4 below summarizes the most optimized conditions found for each of the phosphide skutterudite compounds synthesized in this study as well as their compositions determined by electron microprobe analysis.

Table 4. Experimental procedure for synthesis of phosphide skutterudites by recrystallization from Sn flux

Compound	Mixing molar ratio	Heating rate (°C/h)	Soak temp.(°C)/time	Cooling rate (°C/h)	Microprobe analysis
CoP_3	Co:P:Sn=1:3:25	50	780/1 wk	2	99% $Co_{24.2}P_{75.8}$
$La_{0.24}Co_4P_{12}$	La:Co:P:Sn=1:4:12:50	50	1027/2 days	3	98% $La_{1.5}Co_{24.9}P_{73.6}$
$CeFe_4P_{12}$	Ce:Fe:P:Sn=1:4:20:50	50	777/1 wk	2	97% $Ce_{6.0}Fe_{21.9}P_{72.1}$
$PrFe_4P_{12}$	Pr:Fe:P:Sn=1:4:20:50	50	900/1 wk	2	96% $Pr_6Fe_{21}P_{71}$
$CeRu_4P_{12}$	Ce:Ru:P:Sn=1:4:20:50	50	780/5 days	Furnace cool	96% $Ce_{5.8}Ru_{23.4}P_{70.9}$

B) Direct reaction synthesis

Direct synthesis involves reacting a nominally stoichiometric amount of an elemental powder mixture or compounds at an appropriate temperature and time. In this study, the processing ampoules were made of fused silica with the same dimensions as those used for flux growth. For a given tube volume, the maximum allowable pressure inside was calculated to be about 10 atm for a 1.0 - 1.5 g of charge. In some cases, the starting mixture was placed in a small alumina crucible, which is considered to be more resistant to attack by the rare-earth elements, and then pressed by hand with an alumina rod to provide a better contact among powder particles before being loaded into the processing tube. The fused quartz tubes were evacuated to a pressure of less than 10^{-5} torr, and then sealed before being transferred to the furnace. The reaction temperature varied between 700 - 1050 °C and the soak time was about 5 - 10 days, depending on material systems studied.

In synthesizing CoP_3 with this technique, we found that rapid heating to high temperature (i.e. 950 °C) resulted in densification (sintering) of the synthesized powder. This impeded the

24

reaction between the Co and P and hence skutterudite phase formation. An electron micrograph of such dense solid is shown in Figure 7. The corresponding X-ray diffraction showed that the solid consisted of CoP_3, CoP and Co_2P. It is most likely that the Co_2P is the innermost region of the solid where P did not have enough time to diffuse into and react to form CoP and CoP_3. Later experiments on the same material showed that slower heating rates kept the synthesized material in a low density (unsintered) powder form, leading to complete reaction. All the X-ray peaks of slowly heated procedures corresponded to those of skutterudite phase.
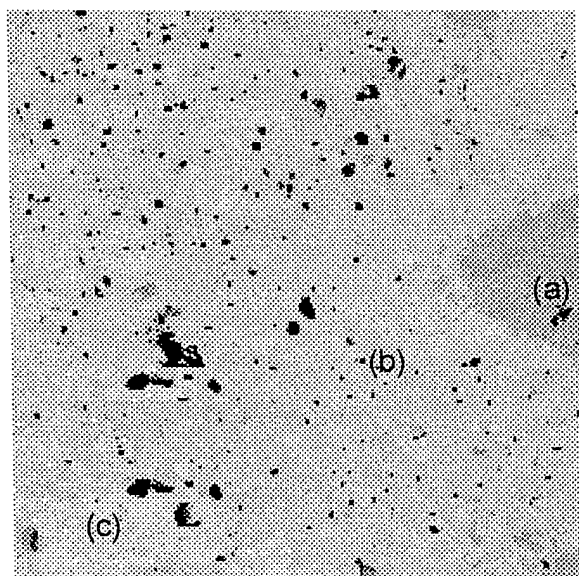

Figure 7. An electron micrograph of a dense solid indicating different regions: (a) CoP_3, (b) CoP, and (c) Co_2P

In order to study the effect of anion substitutions on the properties of CoP_3, the $CoP_{3-x}As_x$ series of solid solutions were prepared. These materials were prepared using two alternative methods. One involved using the binary compounds CoP_3 and $CoAs_3$ as starting components. These two compounds were mixed and heated to a reaction temperature typically around 850 °C. Although lower temperatures were studied, they did not work well for the high phosphorus content solid solutions. The other method involved using a stoichiometric mixture of the pure elements, Co, P and As. The starting powder mixture was ground together and put into a small alumina crucible before being placed into the silica tube. A small amount of excess As and P was added to compensate for any dissociation that might occur. The processing time was typically about one

week. The materials were then analyzed for phase purity and lattice constants (calculated by X-ray diffraction using Si as an internal standard). In Figure 8, a plot of the lattice constant versus composition is shown for the $CoP_{3-x}As_x$ system. The behavior of these alloys (solid curve) deviates slightly from an ideal solid solution. This deviation may be due to the fact that a larger amount of As (to prevent dissociation) was used in some of these experiments. By comparing the experimental results with Vegard's law, it would be expected that the final compositions of several samples would be richer in As than their initial compositions before synthesis. Unfortunately, these samples decomposed during hot-pressing process and the results from electron microprobe analysis could not be used to correctly estimate the stoichiometry of these compounds.
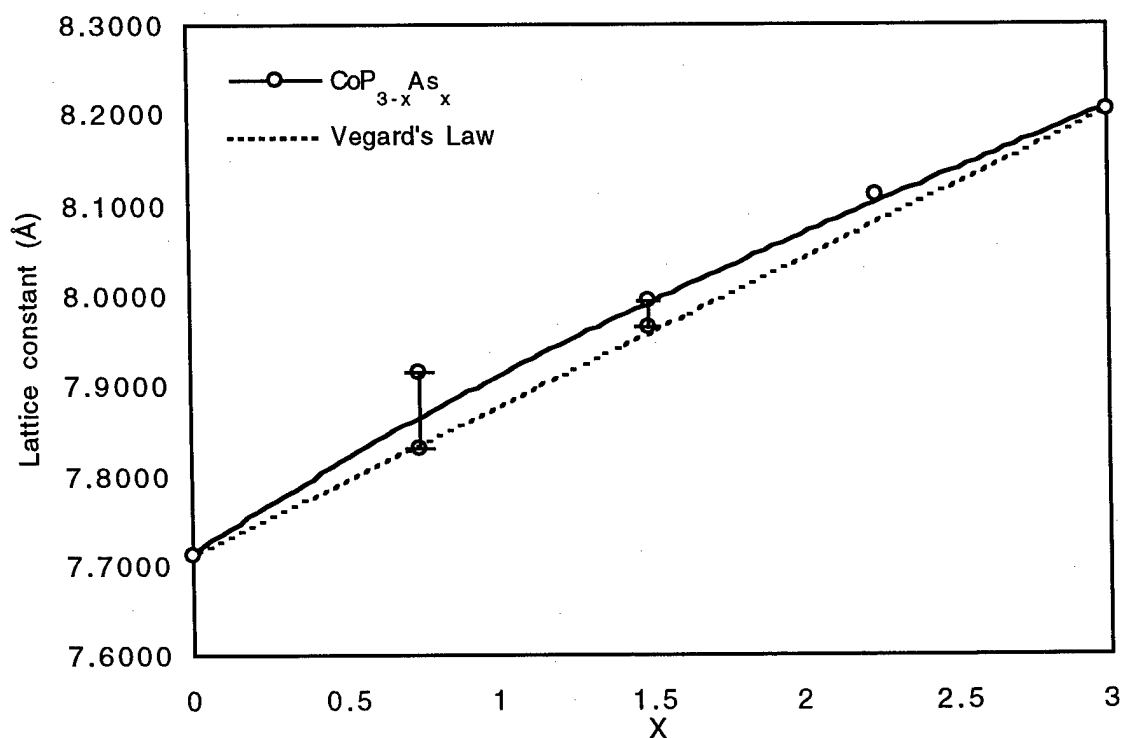

Figure 8. Lattice constants as a function of As concentration in $CoP_{3-x}As_x$ compounds. The deviation from ideal solid solution behavior is shown by a solid curve. X is the amount of As in starting compositions.

To see the effect of both filling atoms as well as disordering on the anion sites, several filled ternary solid solutions were prepared. The starting compositions for the two compounds are

Ce:Co:Si:P = 1:4:3:9 and Ce:Co:Ge:P = 0.3:4:1.2:10.8. The mixtures were placed inside fused silica tubes which were evacuated and sealed. The mixtures were then heated to 950 °C for one week, followed by pelletizing and reannealing at the temperature of up to 1050 °C for another week. This procedure produced single phase materials. It should be mentioned that the differences between initial and final compositions might be due to the loss of some material during the reannealing experiments. The conditions for experimental procedures of these compounds are summarized in Table 5.

Table 5. Experimental procedures for synthesis of phosphide and arsenide skutterudite compounds by direct reaction.

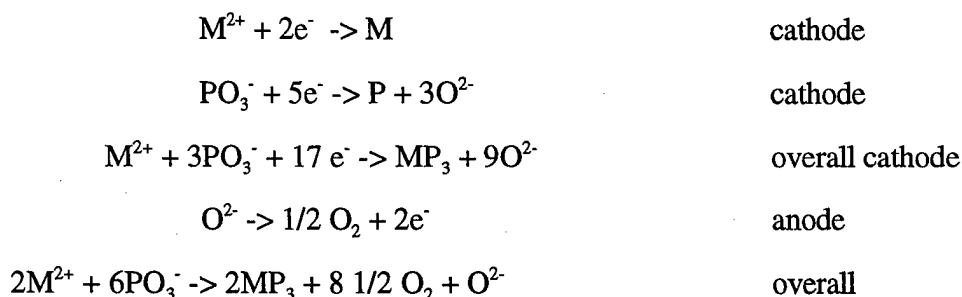| Compound	Mixing molar ratio	Soak temp. (°C)/time	Microprobe analysis
$CeCo_4Si_3P_9$	Ce:Co:Si:P=1:4:3:9	950/5 days	99% $Ce_{5.9}Co_{21.1}Si_{13.3}P_{59.6}$
$Ce_{0.3}Co_4Ge_{1.2}P_{10.8}$	Ce:Co:Ge:P=0.3:4:1.2:10.8	950/5 days	96% $Ce_{1.2}Co_{24.7}Ge_{3.3}P_{70.9}$
CoP_3	Co:P=1:3	600/1 wk	99% $Co_{25.6}P_{74.4}$
$CoAs_3$	Co:As=1:3	600/1 wk	100% $Co_{25.1}As_{74.9}$
$CoP_{1.5}As_{1.5}$	Co:P:As=1.0:1.5:1.5	850/5 days	100% $Co_{25.5}P_{36.2}As_{36.2}$

C) Synthesis by molten salt electrochemical deposition

A possible alternative to direct synthesis or solution growth of the pnictide skutterudites is electrochemical synthesis. Some previous work on the Co-P system was reported by Chene [47] who synthesized a series of cobalt phosphide compounds from melts containing cobalt oxide and sodium metaphosphate. However, he did not report having synthesizing CoP_3. Since, in the past, a large number of other technologically important phosphide compounds such as InP and GaAs have also been electrochemically deposited onto suitable substrates [48-51], it would be very beneficial if the same could be done for skutterudite pnictides.

There are several advantages offered by this techniques when compared to the direct synthesis and solution growth. First, it is normally operated at a relatively low temperature, thereby preventing thermal decomposition and excessive vapor pressure of the pnictides, especially

27

phosphorus. Second, the experiment is essentially unaffected by small changes in temperature since the synthesis is controlled by electrical parameters rather than thermal ones. Third, the technique does not require that either the starting materials or the final products be congruently melting, as it is the case for $CoPn_3$ (Pn=P, As, Sb) which were found to be peritectics [52, 53]. Finally, the total reaction time should be shorter (approximately 2 to 4 days compared with (up to) 2 weeks by the other two techniques).

The reactions taking place at the electrodes during electrolysis can be described by

$$M^{2+} + 2e^- \rightarrow M \qquad\qquad \text{cathode}$$

$$PO_3^- + 5e^- \rightarrow P + 3O^{2-} \qquad\qquad \text{cathode}$$

$$M^{2+} + 3PO_3^- + 17\,e^- \rightarrow MP_3 + 9O^{2-} \qquad\qquad \text{overall cathode}$$

$$O^{2-} \rightarrow 1/2\,O_2 + 2e^- \qquad\qquad \text{anode}$$

$$2M^{2+} + 6PO_3^- \rightarrow 2MP_3 + 8\,1/2\,O_2 + O^{2-} \qquad\qquad \text{overall}$$

The potential (E) for driving the overall reaction can be expressed by the Nernst equation

$$E = \Delta E^0 - \frac{RT}{34F} \ln\left(\frac{[O_2]^{8.5}[O^{2-}]}{[M^{2+}]^2[PO_3^-]^6} \right) \qquad\qquad (7)$$

where ΔE^0 is the difference in standard electrode potentials and the oxygen is included since its partial pressure or, more properly fugacity, is less than 1 atmosphere. Unfortunately, the standard electrode potentials for the molten salt systems that were used to deposit the skutterudites are not known and, therefore, the Nernst equation cannot be use to determine either the reactant concentrations for a given potential or the potential to apply for a given concentration of reactant species. The proper ratio of metal to metaphosphate must be determined empirically. This is the main disadvantage of molten salt electrochemical synthesis.

In our experiments, all electrodepositions were performed in a closed Inconel 600 cylinder fitted with a removable cover sealed with an o-ring. The cover had fittings for two electrodes (anode and cathode), a gas inlet and outlet, a thermocouple, and a view port (Fig. 9). The cylinder was externally heated by a resistance furnace controlled by a PID temperature controller. The melts were contained in a graphite crucible fitted with a baffle to separate the anode and cathode

28

compartments. All experiments were conducted under a flowing nitrogen atmosphere at temperatures between 650 and 660 °C. Current versus voltage (I-V) plots were made before each deposition in order to be sure that the deposition potential was above the last plateau (i.e. threshold potential). The voltages used ranged from 3 - 5 V with currents as high as 1 A. The products were then recovered by dissolving the melts in a recirculating water stream.
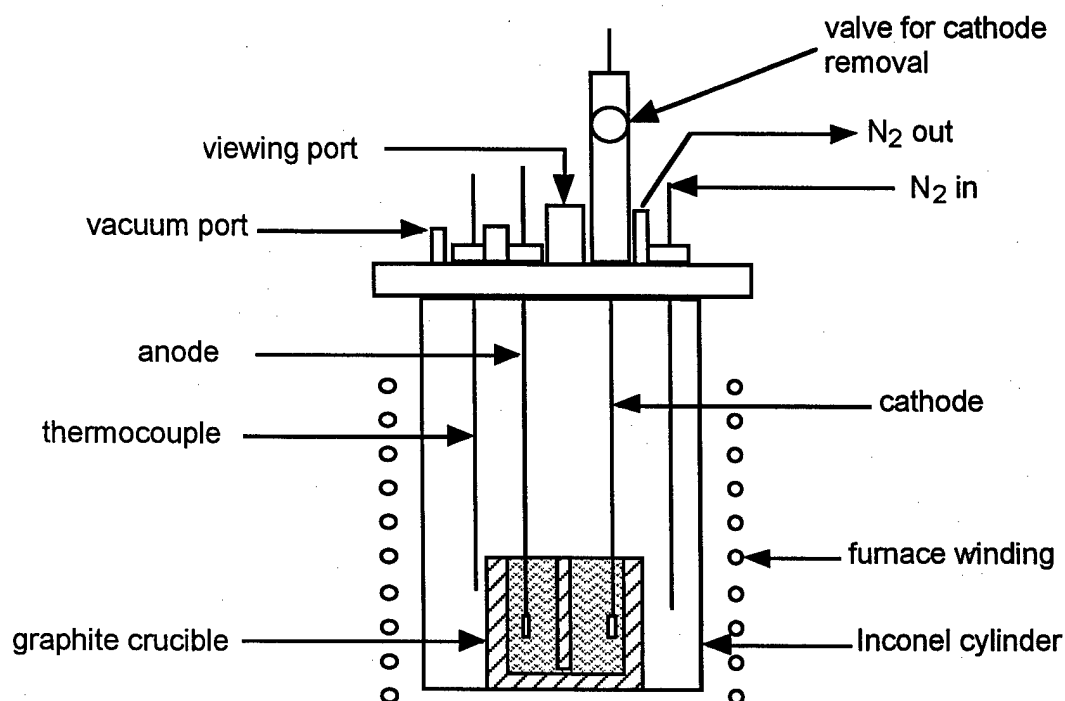

Figure 9. A schematic diagram of electrochemical synthesis experiments

a) CoP₃

The results of Chene's investigations [47] were used to plot the ratio of PO_3^- (metaphosphate) to Co^{+2} in the melt versus the ratio of P to Co in the product and extrapolated to a P:Co ratio of 3:1 to provide a starting point for the CoP_3 melt composition (93.6:1.0). In these electrolysis experiments, graphite electrodes were used. The melt components were CoO and $(NaPO_3)_3$ (sodium trimetaphosphate). Unfortunately, the result was a mixture of Co-P compounds. A systematic study of the effects of melt composition on product stoichiometry was used to find the optimum composition to produce CoP₃. Figure 10 shows a typical I - V plot for

these melts with graphite electrodes. Attempts were also made to grow thin films of CoP_3 on platinum and silver substrates using the same melt composition and a graphite anode.
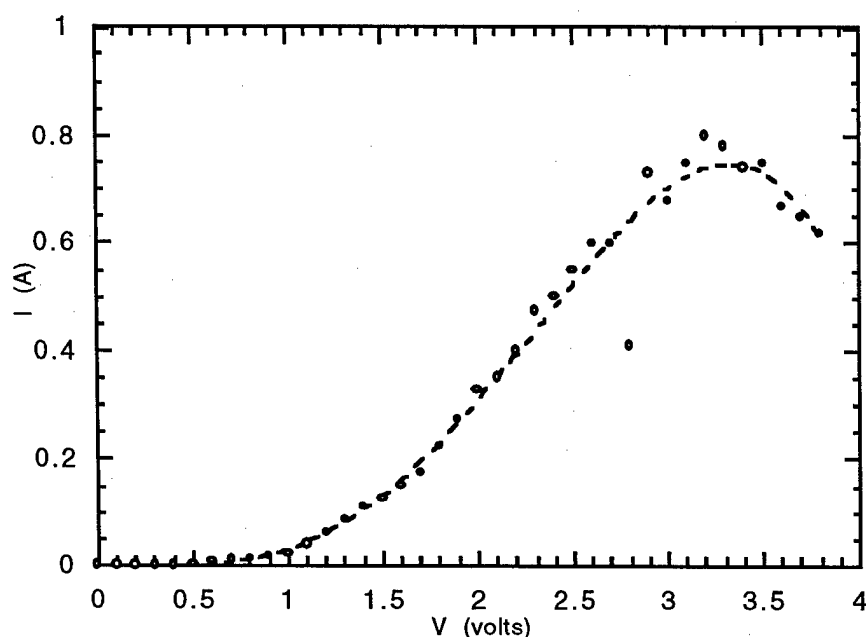

Figure 10. A typical I-V plot for the CoO + $(NaPO_3)_3$ melts with graphite electrodes

Table 6 shows the results of the systematic melt composition changes that lead to the formation of CoP_3. The final melt composition was 99.7 mole % metaphosphate and 1.3 mole%

Table 6. Products versus melt composition for the Co-P system

Melt Composition (mole% PO_3^-)	Products	Amount (% est. from x-ray)	Average P Content (atomic %)
97.6	Co_2P	5	48.8
	CoP	95	
99.0	CoP	50	66.7
	CoP_3	50	
99.3	CoP	12	73.4
	CoP_3	88	
99.7	CoP_3	100	75.0

Co^{+2}. Electrolysis of this melt composition yielded phase pure CoP_3 with slight traces of graphite contamination.

The synthesis of a CoP_3 film on platinum sheet yielded a segmented deposit which may have contained CoP_3, but the major product was found to be platinum phosphide. The subsequent deposition on silver did produce CoP_3 as a film, but of a rather low quality. Due to time constraints, no further experiments on film deposition were done.

b) $CoAs_3$

There were no commercially available metaarsenates (AsO_3^-) to use as a source of As in the molten salt. Our previous experience with GaAs molten salt electrodeposition [50] showed that arsenides can be electrodeposited from melts containing sodium arsenite $(NaAsO_2)$. The only melt composition that was tried for the growth of $CoAs_3$ contained 95 mole% metaarsenite.

The electrolysis product of this melt contained 89.5% $CoAs_3$ and 10.5% $CoAs_2$ (estimated from x-ray diffraction patterns). There was evidence that some of the arsenite had evaporated from the melt during the two day experiment. There have been no further attempts to synthesize $CoAs_3$, but it is obvious that the melt composition should be modified. Not only will the ratio of arsenite to cobalt ion have to be changed, but other components will have to be added to the melt to reduce the melting temperature as was done with the melts for GaAs [50].

c) $CoSb_3$

Initially we were not able to find any commercially available metaantimonate or metaantimonite so we used a melt containing sodium carbonate (Na_2CO_3) and antimony oxide (Sb_2O_3) which would react to form the antimonite. The melt was nominally 95% metaantimonite and was electrolyzed with graphite electrodes.

The electrolysis products contained metallic antimony (70.4%) and $CoSb_3$ (29.6%). Again, the melt composition will need to be adjusted to produce phase pure material. A different source of

antimony, potassium hexahydoxyantimonate, has been found, but no further experiments were performed due to limited time and funding.

Nevertheless, we have shown for the first time that the binary cobalt pnictide skutterudites can be synthesized by molten salt electrolysis. While cobalt triphosphide was obtained as a single phase product, the arsenide and antimonide process have not yet been optimized. The only barrier to obtaining these materials as a single product is the adjustment of the melt composition. From our thin film experiments, finding a suitable substrate is also challenging since these synthesized compounds did not seem to adhere well to the surface of electrode materials and the pnictogens, especially phosphorus, seemed to react with most of the elements in the Periodic Table to form phosphides at these elevated temperatures.

Our results with CoP_3 are rather interesting compared with Chene's [47] work. He reported obtaining CoP_2 as one of the products of his electrochemical studies and there is an x-ray diffraction pattern for it. Even though a range of compounds from Co_2P to CoP_3 was deposited in the current experiments, there was no evidence for the formation of a CoP_2 compound as reported by Chene [47], despite similar synthesis conditions and temperature ranges used. The Co-P phase diagram [54] is incomplete due to the lack of data in the region of high phosphorus content. The analogous phase diagrams for Co-As [52] and Co-Sb [53] do show the di- and tri-pnictide compounds forming as peritectics. It is a reasonable assumption that the phosphide would behave similarly and it is puzzling that the diphosphide was not obtained. The only conclusion that can be reached at this point is that this phase may not be thermodynamicly stable. The difficulties related to the synthesis of the CoP_2 phase by direct synthesis from the pure elements was reported by Donohue [55]. He also reported the synthesis of this phase using a Ge flux at high temperature and pressure. It is unfortunate that the scope of this research did not allow us to further investigate the electrochemistry in this region of the phase diagram.

32

D) Thermoelectric Property Measurements

The experimental procedures in this section were preestablished and carried out at the Jet Propulsion Laboratory. After the materials were synthesized (normally as powder), they were then hot-pressed in graphite dies into dense samples, 2.0 mm long and 12.0 mm in diameter. The hot-pressing was conducted at a pressure of about 20,000 psi and at temperature of 1173 K for about 2 hours under an argon atmosphere. Microprobe analysis (MPA) was performed on these samples to determine their atomic composition using a JEOL JXA-733 electron superprobe operating at 20×10^3 Volts (V) of accelerating potential and 25×10^{-9} Amperes (A) of probe current. Pure elements and compounds were used as standards and x-ray intensity measurements of peak and background were conducted by wavelength dispersive spectrometry. The density of the samples was calculated from the measured weight and dimensions of the samples.

Samples in the form of disks (typically 1.0 mm thick and 12.0 mm diameter) were cut from the cylinders using a diamond saw (perpendicular to the pressing direction) for electrical and thermal transport property measurements. All samples were characterized at room temperature by Seebeck coefficient, Hall effect and electrical resistivity measurements. High temperature resistivity, Hall effect, Seebeck coefficient, thermal diffusivity, and heat capacity measurements were also conducted between room temperature and about 900K. The electrical resistivity (ρ) was measured using the Van der Paw technique with a current of 100 mA using a special high temperature apparatus [56]. The Hall coefficient (R_H) was measured in the same apparatus with a constant magnetic field value of $\sim 10,400$ Gauss. The carrier density was calculated from the Hall coefficient, assuming a scattering factor of 1.0 in a single carrier scheme, by $p = 1/R_H e$, where p is the density of holes, and e is the electron charge. The Hall mobility (μ_H) was calculated from the Hall coefficient and the resistivity values by $m_H = R_H/r$. Errors were estimated to be $\pm 0.5\%$ and $\pm 2\%$ for the resistivity and Hall coefficient data, respectively. The Seebeck coefficient (α) of the samples was measured on the same samples used for electrical resistivity and Hall coefficient measurements using a high temperature light pulse technique [57]. The error of the Seebeck

33

coefficient measurement was estimated to be less than $\pm$ 3%. The heat capacity and thermal diffusivity were measured using a flash diffusivity technique [58]. The thermal conductivity (λ) was calculated from the experimental density, heat capacity, and thermal diffusivity values. The overall error in the thermal conductivity measurements was estimated to be about $\pm$ 10%. In addition, electrical resistivity and Seebeck coefficient measurements were conducted between 2K and 300K for some compounds of interest. A Quantum Design PPMS was used for low temperature thermopower and resistivity measurements. Au-Fe7% vs. chromel thermocouples were used to measure both the temperatures and Seebeck voltage across the sample. The Seebeck coefficient was then referenced to copper by subtracting the Seebeck voltage of the thermocouple wires, with respect to copper.

E) Theoretical Treatment of the Effect of Porosity on Thermal Conductivity

In a number of phosphide based skutterudite materials, the density of hot-pressed samples was not optimal. Therefore, to take sample porosity into account in figure of merit calculations, the Maxwell and Rayleigh relationships [59, 60] was used:

$$\frac{k_s}{k} = \frac{1 + 0.5P}{1 - P} \qquad (8)$$

where k_s = thermal conductivity for theoretically dense sample, k = measured thermal conductivity, and P = porosity. Although this correction may not correspond to the actual values of the samples, it can at least provides a more accurate calculation.

IV. RESULTS AND DISCUSSION

A. Effect of La Atom Filling in CoP_3 Skutterudite

Fornari and Singh [62] suggested in their recent energy band calculation of CoP_3 that n-type conduction seems to be more favorable for these compounds. This produces a large Seebeck coefficient which is related to the heavy mass structure (or small curvature) of the conduction band minimum compared with the light mass structure (or large curvature) of the valence band maximum. Our La-Co-P experiment was designed to provide some experimental data regarding the relationship between the electrical properties and the calculated band structure . It should be mentioned that although it is preferable to be able to see the property change as a function of La concentration in CoP_3 lattice, changing the stoichiometry of La-filled CoP_3 is difficult by the technique used to synthesized these materials [40].

Table 7 compares some room temperature properties of CoP_3 and $La_{0.24}Co_4P_{12}$. Assuming that the lattice distortion produced by La atoms did not significantly change the energy band of CoP_3, the results indicate that Fermi level moves passed the bottom of the conduction band, thus rendering n-type conduction in $La_{0.24}Co_4P_{12}$. The larger Seebeck coefficient as well as the lower Hall mobility suggests a larger value of carrier effective mass, in agreement with the band structure calculation [62].

Table 7. Some room temperature properties of CoP_3 and $La_{0.24}Co_4P_{12}$

	Units	CoP_3	$La_{0.24}Co_4P_{12}$
Lattice constant	Å	7.7073	7.7375
Percentage of the theoretical density	%	87	78
Type of conductivity		p	n
Electrical resistivity	mΩcm	0.26	0.61
Seebeck coefficient	μV/K	15	-41
Hall carrier concentration	10^{19}/cm^3	3.26	82
Hall mobility	cm^2/Vs	748	12.6
Thermal conductivity	mW/cmK	185	28

The electrical resistivity as a function of temperature for the two compounds is shown in Fig. 11. The resistivity for the La-filled compound increases with increasing temperature which confirms the hypothesis that the Fermi level lies above the conduction band minimum and it seems that this material is a degenerate, n-type semiconductor. CoP_3, on the other hand, shows semiconducting behavior from low temperature up to about 350 K, then its resistivity slightly increases with increasing temperature. This behavior seems to agree with the band calculation by Llunell et al. [63], who reported an indirect bandgap of 0.07 eV and a relatively large pseudogap of 1.26 eV. Figure 12 shows the variation of the Seebeck coefficient with temperature. Above room temperature, the Seebeck coefficient of CoP_3 is positive and increases with temperature to a maximum value of about 35 μV/K near 600 K. The Seebeck coefficient of $La_{0.24}Co_4P_{12}$ is negative and its magnitude (absolute value) increases with increasing temperature. The maximum value is about 60 μV/K near 850 K which was the maximum measurement temperature.

The reduction of the thermal conductivity of $La_{0.24}Co_4P_{12}$ compared with that of CoP_3 is shown in Figure 13. It seems that La atoms in CoP_3 lattice provide additional phonon scattering. The difference in the thermal conductivity more than compensates for a slight difference in sample density. Therefore, with lower thermal conductivity and larger Seebeck coefficient, ZT values of the filled ternary compound are larger than those of CoP_3 as shown in Fig. 14.

This experiment shows that highly doped n-type phosphide skutterudite can be produced and the properties agrees well with those of n-type antimonide skutterudites where large Seebeck coefficient and low thermal conductivity were reported [64].
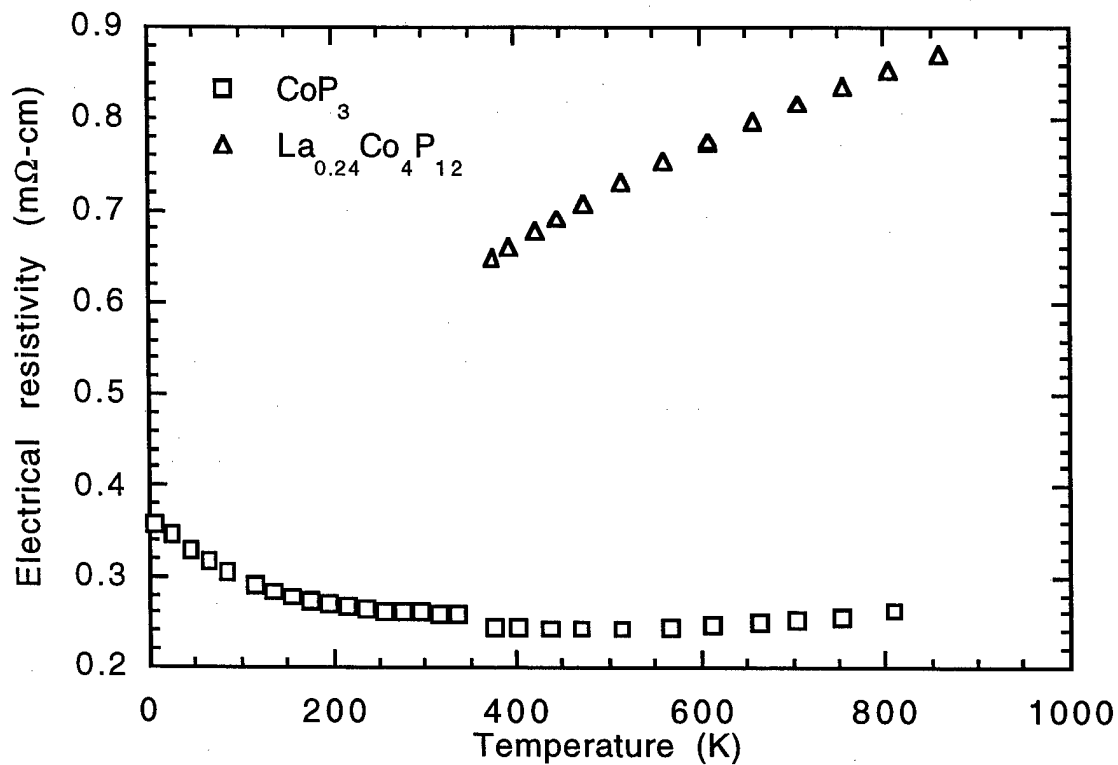
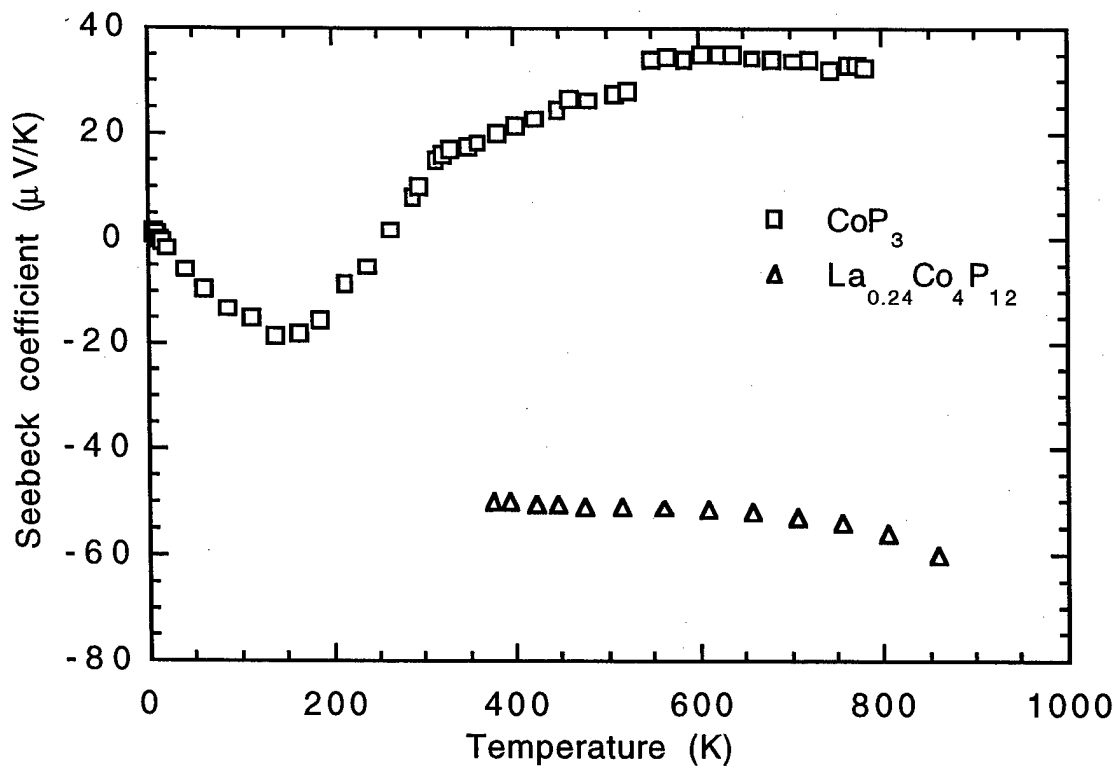Figure 11. Electrical resistivity as a function of temperature

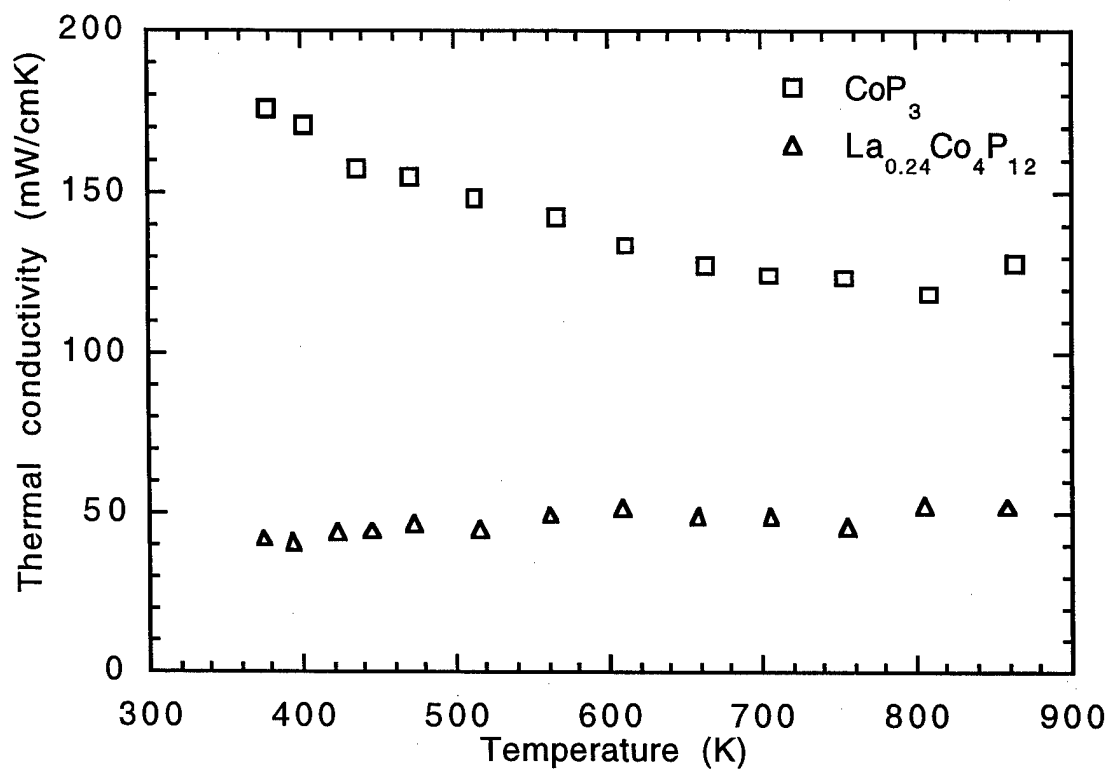Figure 12. Seebeck coefficient as a function of temperature

37

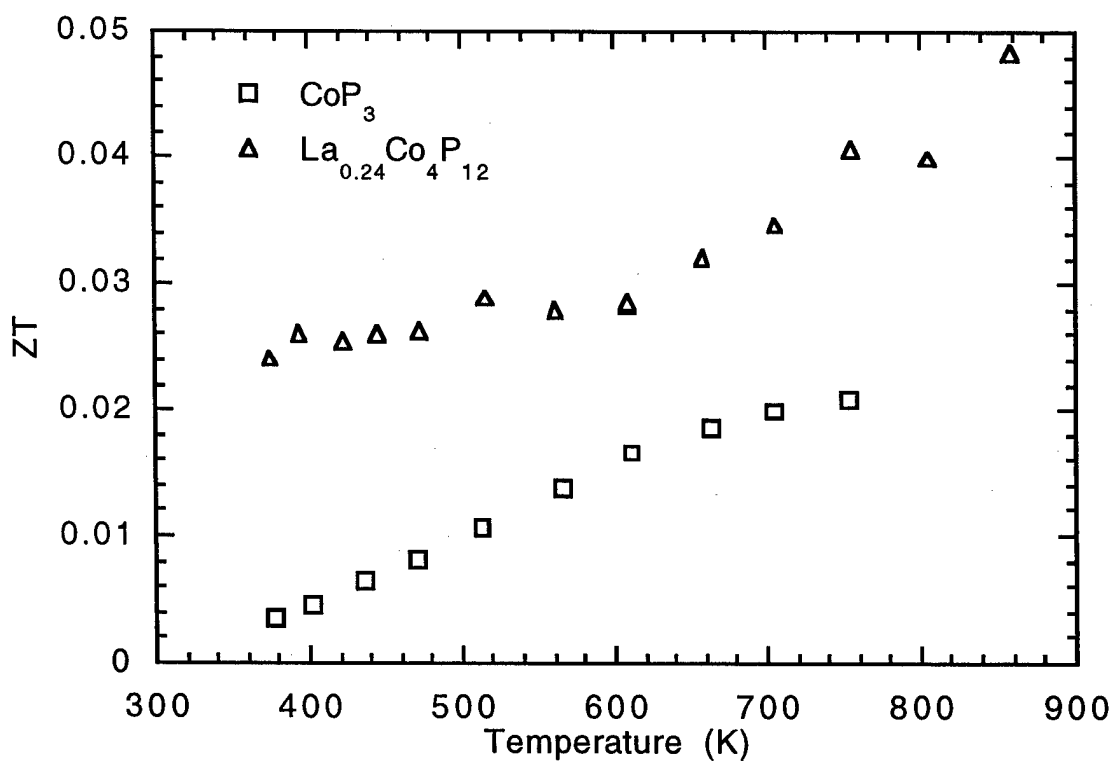Figure 13. Thermal conductivity as a function of temperature

Figure 14. ZT values as a function of temperature

B. Thermoelectric Properties of Some Filled Ternary Compounds

This study focused on the effect of changing different rare-earth atoms and transition metal atoms in the filled ternary compounds. Table 8 lists some physical properties of $CeFe_4P_{12}$, $PrFe_4P_{12}$ and $CeRu_4P_{12}$ at room temperature. All of these materials exhibit p-type conduction. A large carrier concentration was observed for $PrFe_4P_{12}$ compared with the other two compounds. This material has a metallic behavior, as confirmed by the increase in electrical resistivity with temperature (Fig. 15).

Table 8. Some room temperature properties of several filled ternary phosphide skutterudites

	Units	$CeFe_4P_{12}$	$PrFe_4P_{12}$	$CeRu_4P_{12}$
Lattice constant	Å	7.7917	7.8149	8.0419
Percentage of the theoretical density	%	99	91	87
Type of conductivity		p	p	p
Electrical resistivity	mΩcm	20.5	0.76	11.99
Seebeck coefficient	μV/K	58	13	125.6
Hall carrier concentration	10^{19}/cm^3	1.42	316	18
Hall mobility	cm^2/Vs	24.9	2.6	6
Thermal conductivity	mW/cmK	140	79	86[*]

*extrapolate value

From the same figure, the cerium compounds shows similar semiconducting behavior above 200 K. However, below this temperature, the electrical resistivity of $CeFe_4P_{12}$ decreased while that of $CeRu_4P_{12}$ increased to an insulating range. This behavior seems to correspond well to the low temperature measurements of the Seebeck coefficient (Fig. 16). In the case of $CeFe_4P_{12}$, the temperature corresponding to the maximum resistivity value is near the temperature where the Seebeck coefficient changes from positive to negative values. It is possible that some extrinsic conduction plays a role at this temperature range. The large value of the Seebeck coefficient in

$CeRu_4P_{12}$ agrees with high electrical resistivity observed. At higher temperatures, the Seebeck coefficient of $CeRu_4P_{12}$ decreases while that of $CeFe_4P_{12}$ increases with temperature. The Seebeck coefficient of $PrFe_4P_{12}$ is relatively small and increases slightly with temperature.

The thermal conductivity data for these compounds are shown in Fig. 17. The thermal conductivities of $CeRu_4P_{12}$ and $PrFe_4P_{12}$ are relatively independent of temperature, while that of $CeFe_4P_{12}$ shows a strong (1/T) dependence of temperature. Below about 660 K, the thermal conductivity of the former two compounds are lower than that of $CeFe_4P_{12}$. Above this temperature, the thermal conductivity of $CeFe_4P_{12}$ decreases more rapidly and above 720 K, it becomes lower than the other two compounds. This behavior suggests strong phonon-phonon scattering at high temperature for $CeFe_4P_{12}$ due to the rattling of Ce atoms.

The ZT values of these compounds are plotted in Fig. 18. A sharp increase in ZT values is observed for $CeFe_4P_{12}$ while the values for the other two materials are relatively small and increases slightly with temperature. This behavior is a result of an increase in the ratio of electrical conductivity to thermal conductivity as well as an increase in the Seebeck coefficient. It seems that Ce and Fe play a crucial role in producing high ZT in skutterudite compounds, as is the case for the state-of-the-art $CeFe_4Sb_{12}$. The effect of larger unit cells in the case of $PrFe_4P_{12}$ and $CeRu_4P_{12}$ can lower the thermal conductivity but the electrical properties need to be optimized.
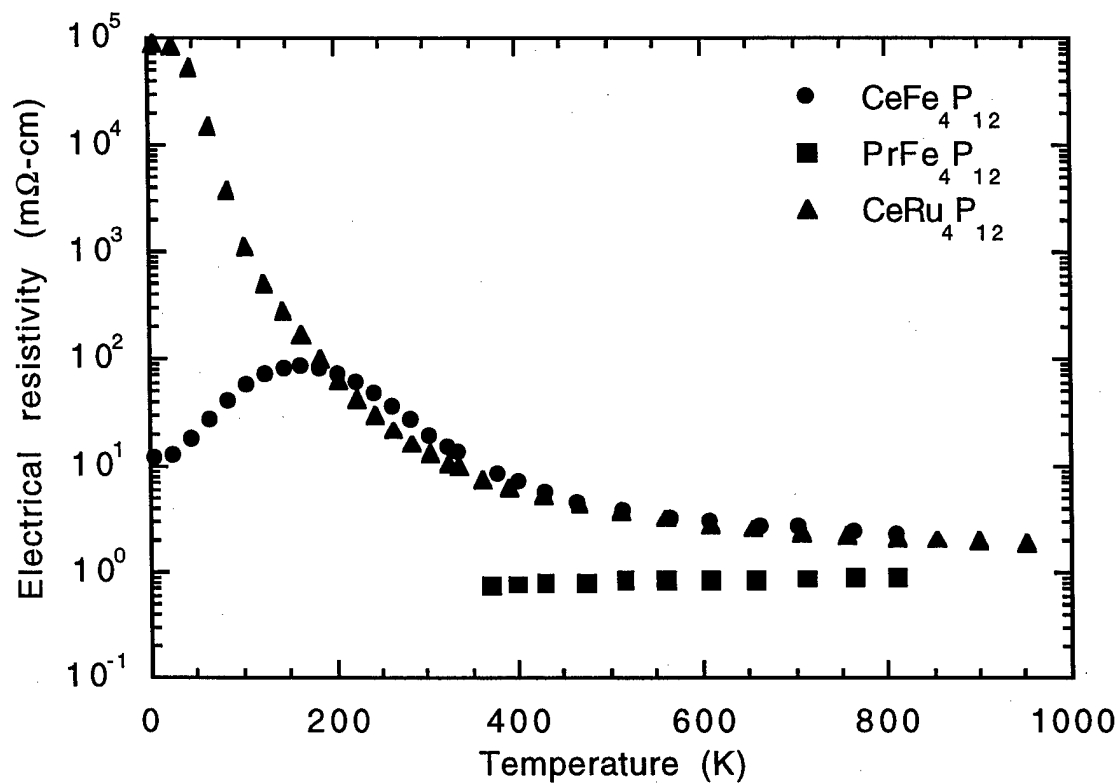
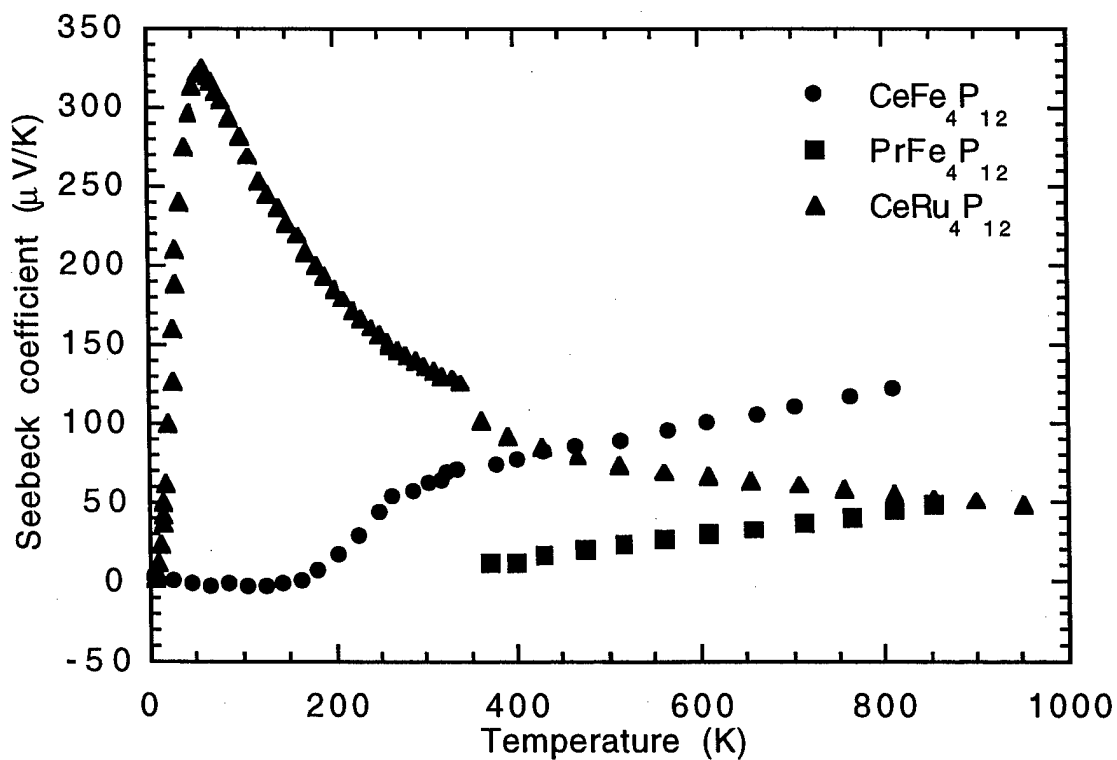Figure 15. Electrical resistivity as a function of temperature

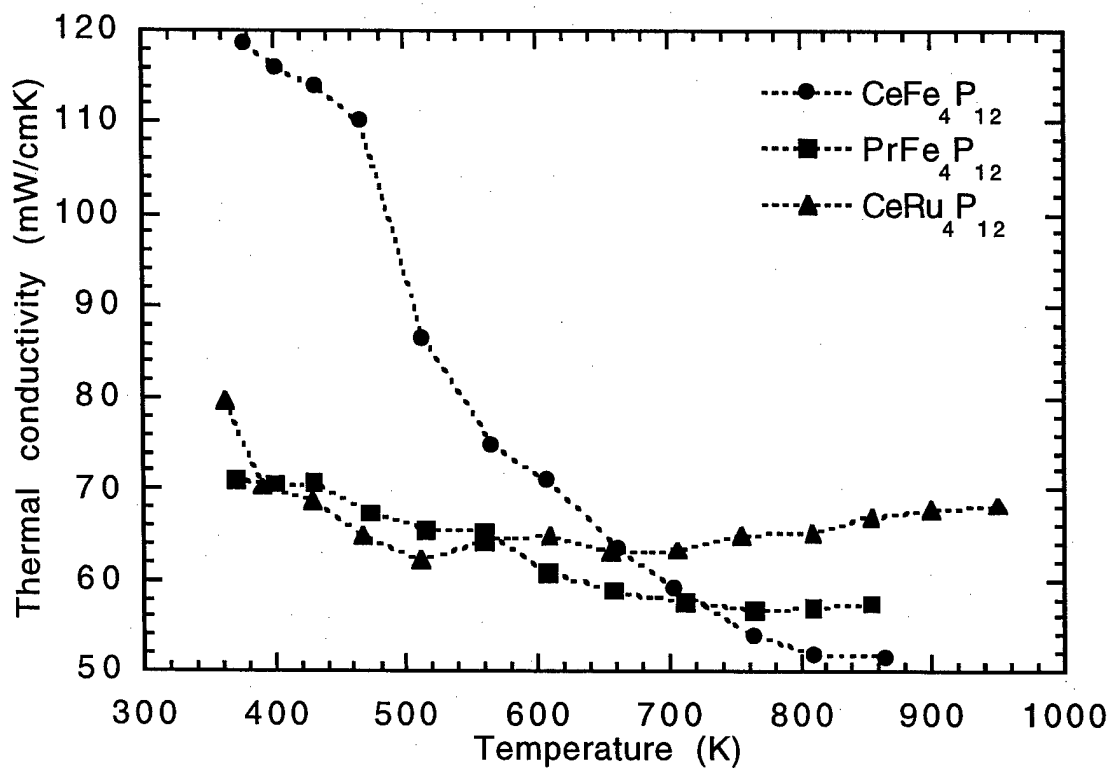Figure 16. Seebeck coefficient as a function of temperature

41

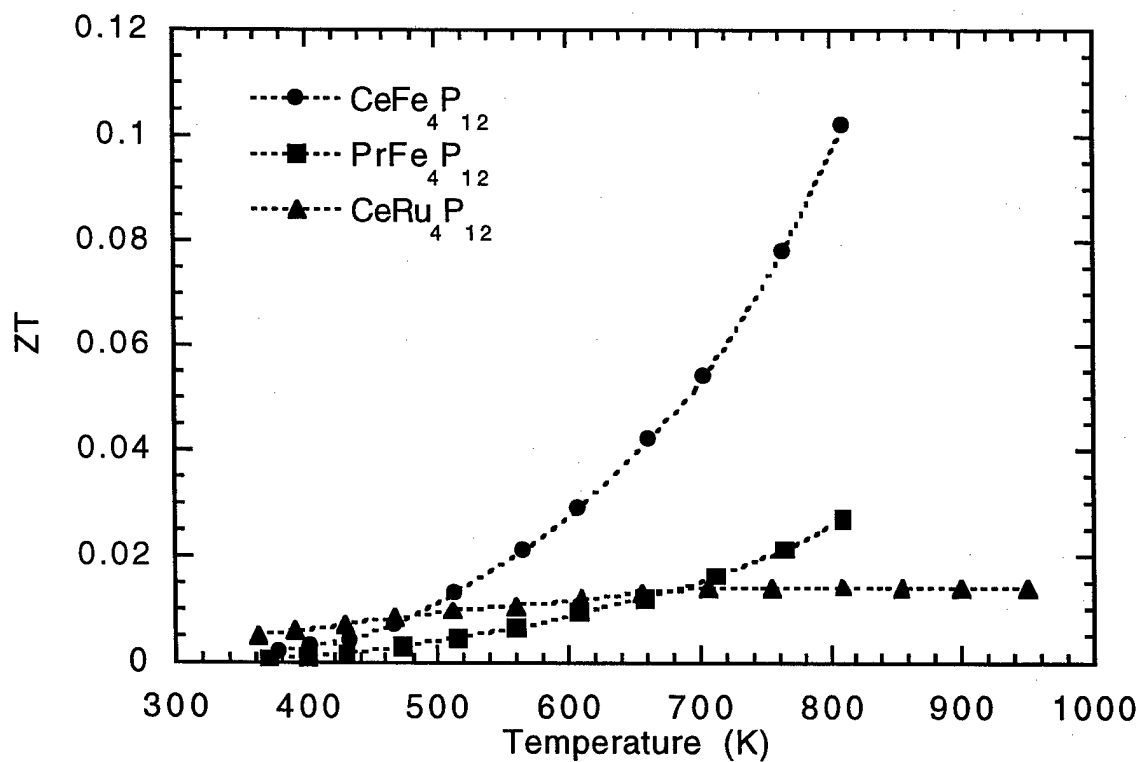Figure 17. Thermal conductivity as a function of temperature

Figure 18. ZT as a function of temperature

C. Studies of Anion Substitution in $CoP_{3-x}As_x$ System

This study follows the theoretical treatment of Ioffe [7] that, by substituting isovalent atoms in a compound, the thermoelectric figure of merit may be improved. This proposition based on the lowering of the thermal conductivity by lattice disorder, provided that electrical properties are not significantly affected by such substitution. In the $CoP_{3-x}As_x$ system, it has been reported that a complete solid solution can be obtained [65]. This provided us with an opportunity to study how the properties can be tuned by varying composition. Although we successfully synthesized three solid solutions with varied compositions, two of those were lost in the hot-pressing process. Nevertheless, the solid solution which we could make property measurements on may be near the composition where the effect of lattice disorder on phonon scattering is maximized, as in the case of GaAs-InAs [66] or Si-Ge alloys [67] whose minimum lattice thermal conductivities were obtained near 50-50 composition. The room temperature properties of this solid solution as well as those of the end compounds are listed in Table 9. All compounds exhibited p-type conduction. Most properties of the solid solution fell between the two end compounds, except for the Seebeck coefficient which has larger values than CoP_3 and $CoAs_3$. Another surprising trend was that $CoAs_3$ seems to be more insulating than CoP_3. This seems to be in contrast to most compounds where the larger anions usually render the material more metallic than those formed with smaller anions [68]. This suggests a stronger bonding in the arsenide compound than that of the phosphides or antimonides.

Figure 19 shows the electrical resistivity as a function of temperature of the three compounds. The activation energy was calculated to be 0.043 eV for CoP_3, 0.066 eV for $CoP_{1.5}As_{1.5}$, and 0.26 eV for $CoAs_3$. The value for CoP_3 is in agreement with the values of 0.045 eV determined from its plasma frequencies [24] and 0.042 eV obtained from infrared transmission spectra [69]. The value for $CoAs_3$ is also in close agreement with the value of 0.21 eV obtained from the temperature dependence of the plasma resonance frequency [24]. The value for the solid solution should then fall between these two end compounds as may be expected.

Table 9. Some room temperature properties of $CoP_{3-x}As_x$ system

	Units	CoP_3	$CoAs_3$	$CoP_{1.5}As_{1.5}$
Lattice constant	Å	7.7073	8.2045	7.9645
Percentage of the theoretical density	%	97.5	99.6	86.5
Type of conductivity		p	p	p
Electrical resistivity	mΩcm	0.47	8.40	1.57
Seebeck coefficient	μV/K	30.4*	25.7	89.3
Hall carrier concentration	$10^{19}/cm^3$	2.7	0.057	0.5
Hall mobility	cm^2/Vs	493	1317	784
Thermal conductivity	mW/cmK	258*	125*	44*

*extrapolate values

Figure 20 shows the dependence of the Seebeck coefficient on temperature. Although it was expected that the value for $CoAs_3$ would be the highest among the three materials studied, considering its lower carrier concentration, this was not the case. The results showed that the solid solution has largest Seebeck coefficient at all temperatures. This indicates the possibility of band structure modification in such a way that Seebeck coefficient can be improved. The details of such discussion must be theoretically derived in order to compliment the experimental results.

The thermal conductivity as a function of temperature is shown in Figure 21. As may be expected, the effect of lattice disorder in the solid solution tends to lower the lattice thermal conductivity in semiconducting materials as suggested by Ioffe [7]. With an increase in Seebeck coefficient and improved σ/κ ratio, the ZT values are thus highest in the solid solution as plotted in Figure 22. This study shows a case where an improvement in thermoelectric properties is obtained when isovalent anion atoms are substituted into original material. This is partly due to an unexpected increase in Seebeck coefficient.
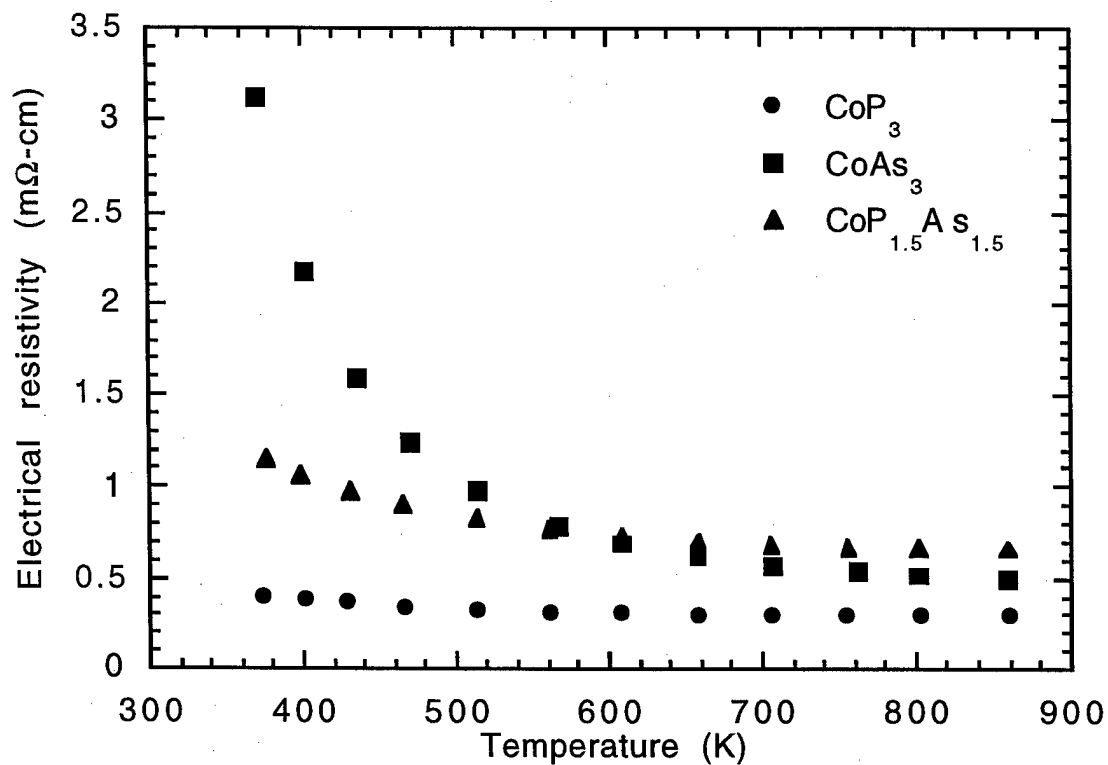
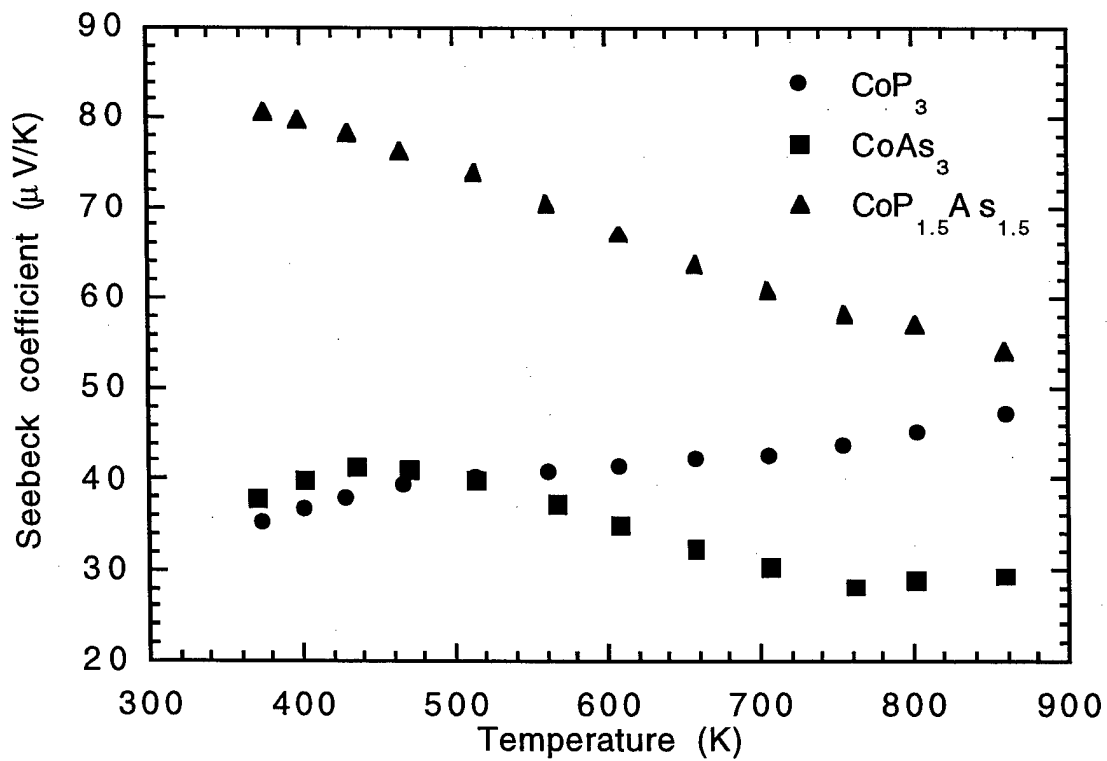Figure 19. Electrical resistivity as a function of temperature

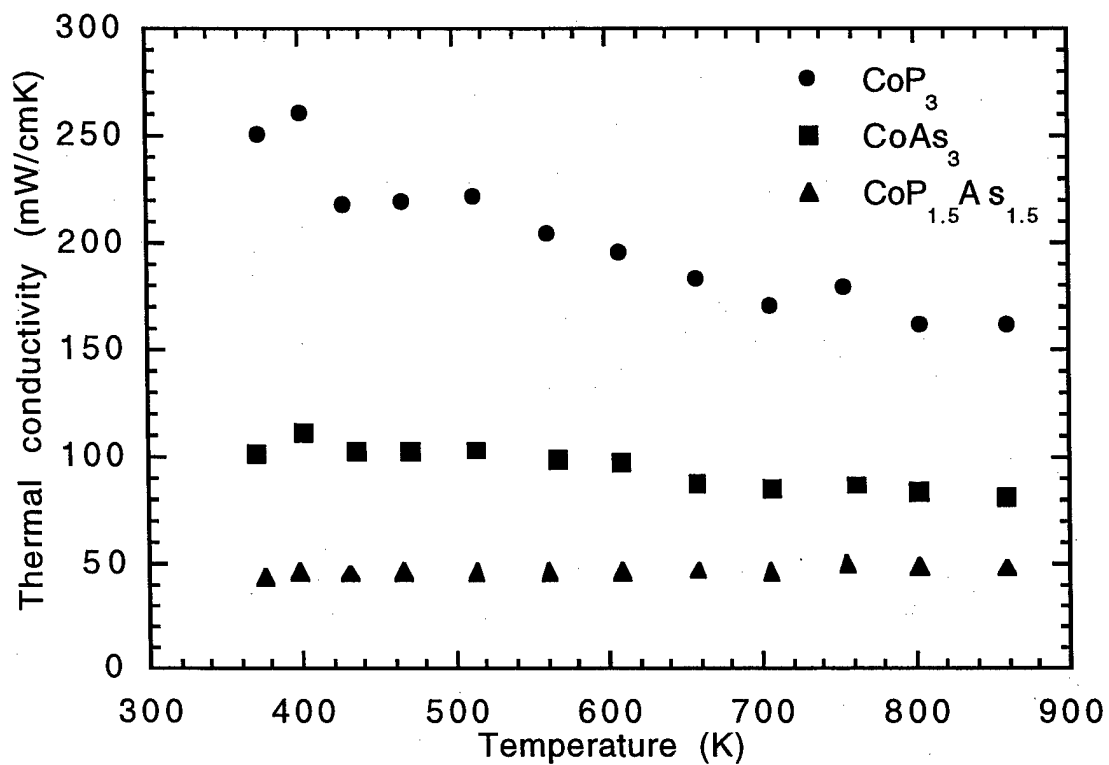Figure 20. Seebeck coefficient as a function of temperature

45

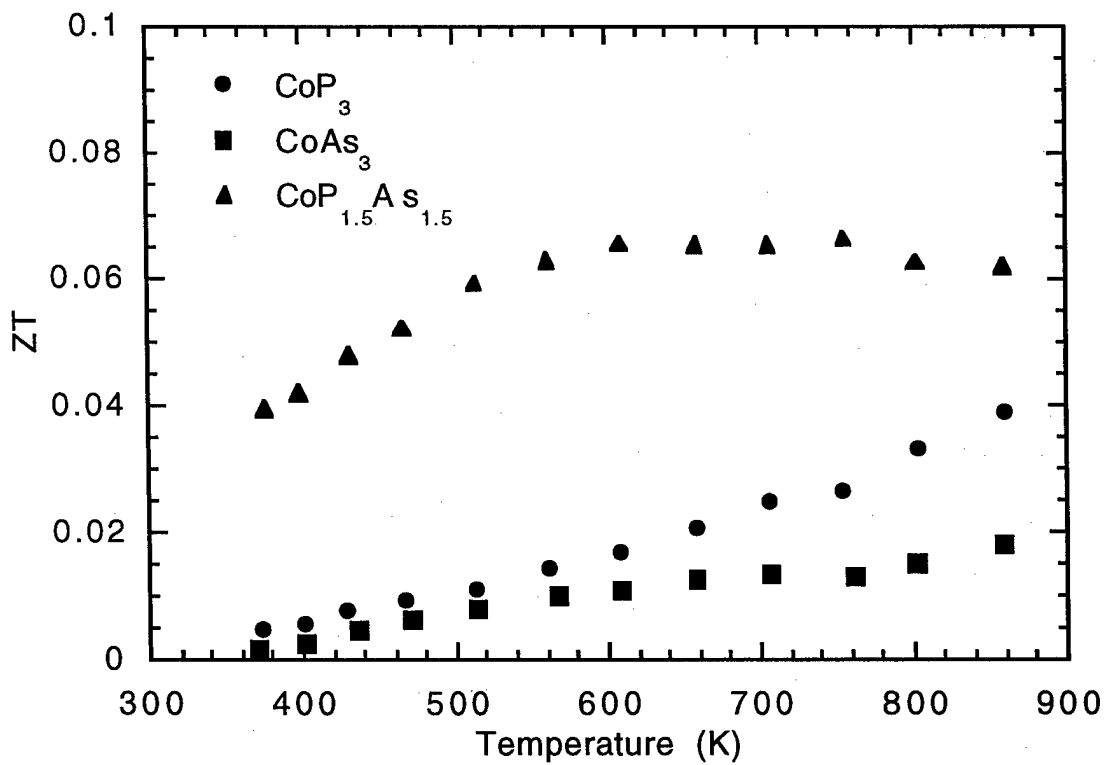Figure 21. Thermal conductivity as a function of temperature

Figure 22. ZT as a function of temperature

D. Thermoelectric Properties of Some Multinary Compounds

In this study, both filling atoms and anion substitution have been attempted on the two compounds listed in Table 10 below. The actual compositions of these compounds are listed in the experimental section. The Si-based compound gives n-type conduction while the Ge-based compound exhibits p-type conduction. The properties of these two compounds at room temperature seems not to be much different.

Table 10. Room temperature properties of some multinary compounds

	Units	$CeCo_4Si_3P_9$	$Ce_{0.3}Co_4Ge_{1.2}P_{10.8}$
Lattice constant	Å	7.8368	7.7433
Percentage of the theoretical density	%	83.0	96.0
Type of conductivity		n	p
Electrical resistivity	$m\Omega cm$	1.4	0.46
Seebeck coefficient	$\mu V/K$	-10.6	21.7
Hall carrier concentration	$10^{19}/cm^3$	13.5	14.1
Hall mobility	cm^2/Vs	32.9	95.5
Thermal conductivity	mW/cmK	23.3	22.6

Figure 23 and 24 show electrical properties of these compounds as a function of temperature. Both materials exhibited metallic conductivity where the resistivity increased slightly with temperature. The Si-based compound gave an increase in (absolute values of) the Seebeck coefficient with increasing temperature while the Ge-based compound only shows a slight increase with temperature up to about 600 K, then decreases.

The thermal conductivity as a function of temperature is shown in Fig. 25. The difference in their values lie in the difference in sample density as well as the amount of Ce filling and lattice disorder. Nevertheless, these two compounds had small ZT values as shown in Fig. 26.
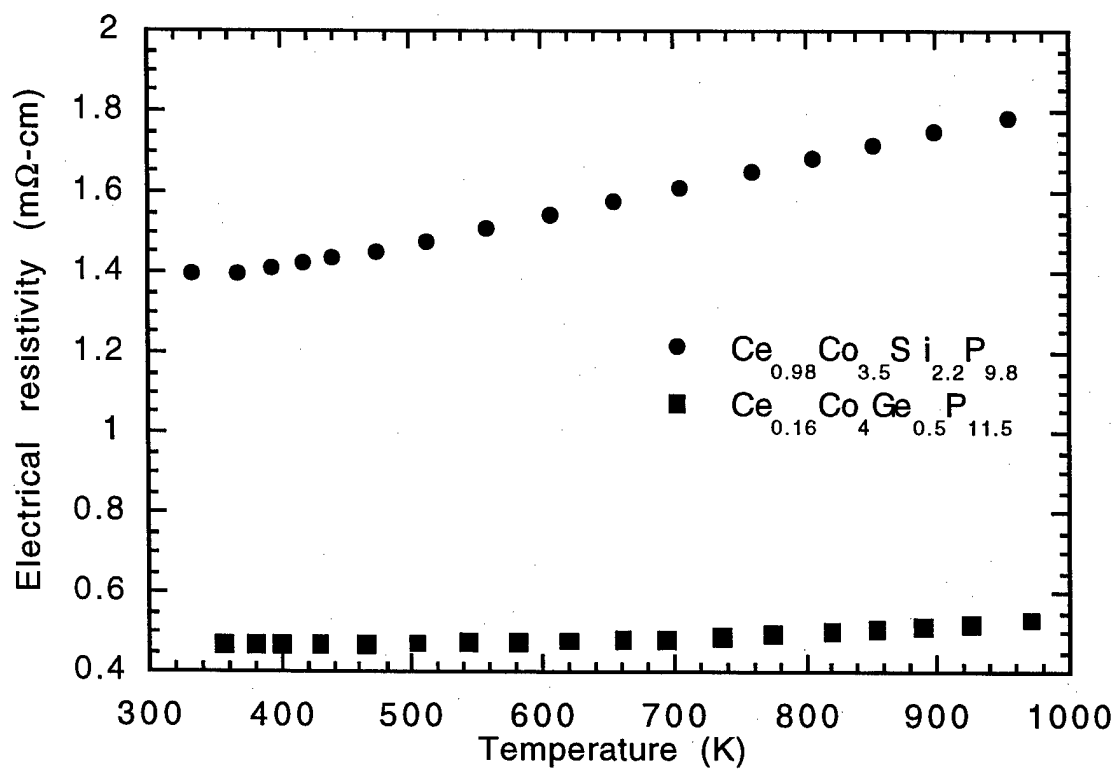
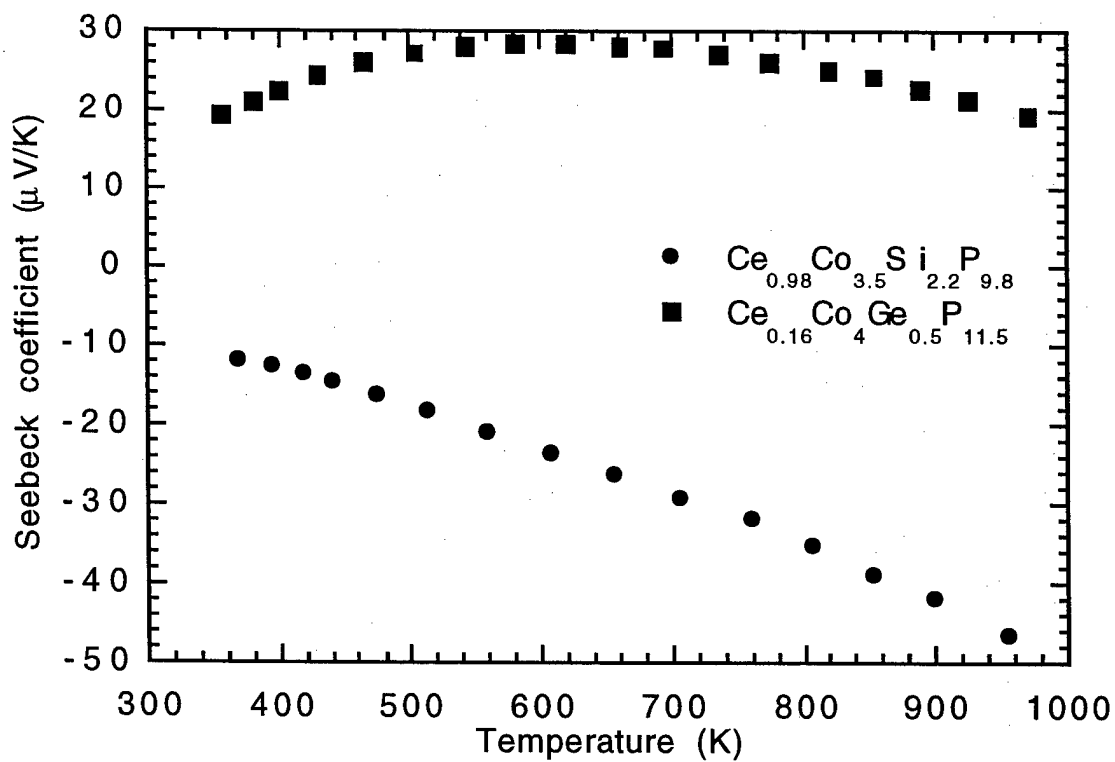Figure 23. Electrical resistivity as a function of temperature

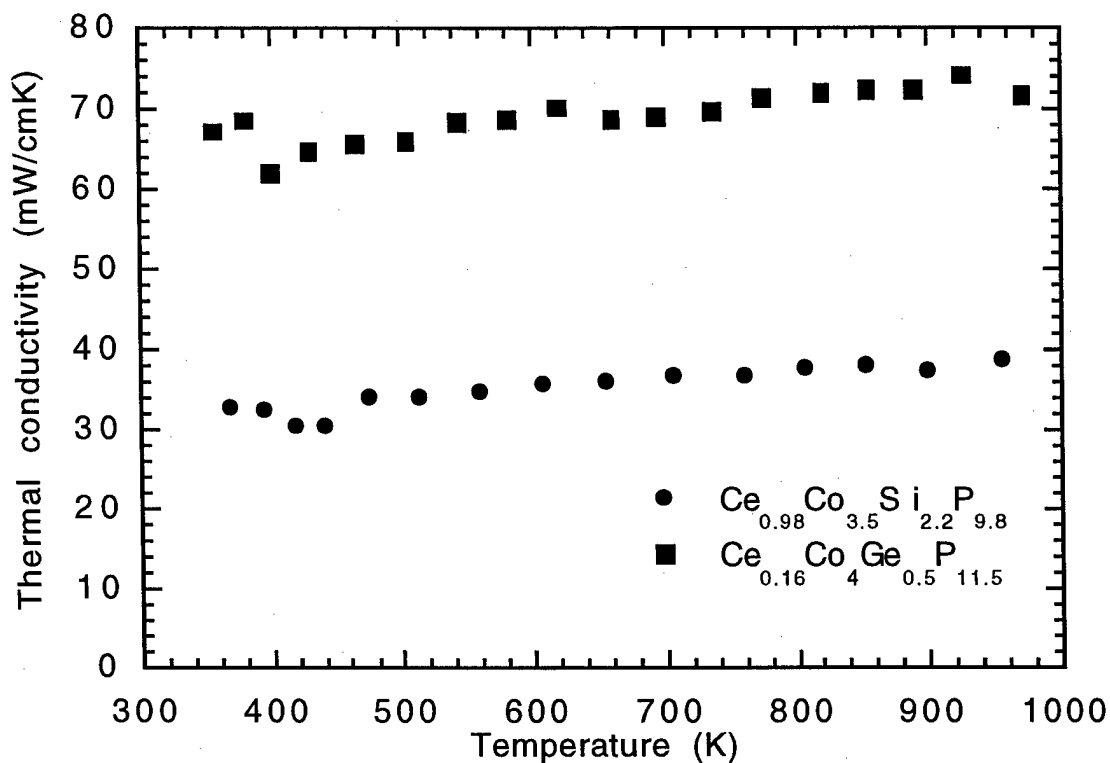Figure 24. Seebeck coefficient as a function of temperature

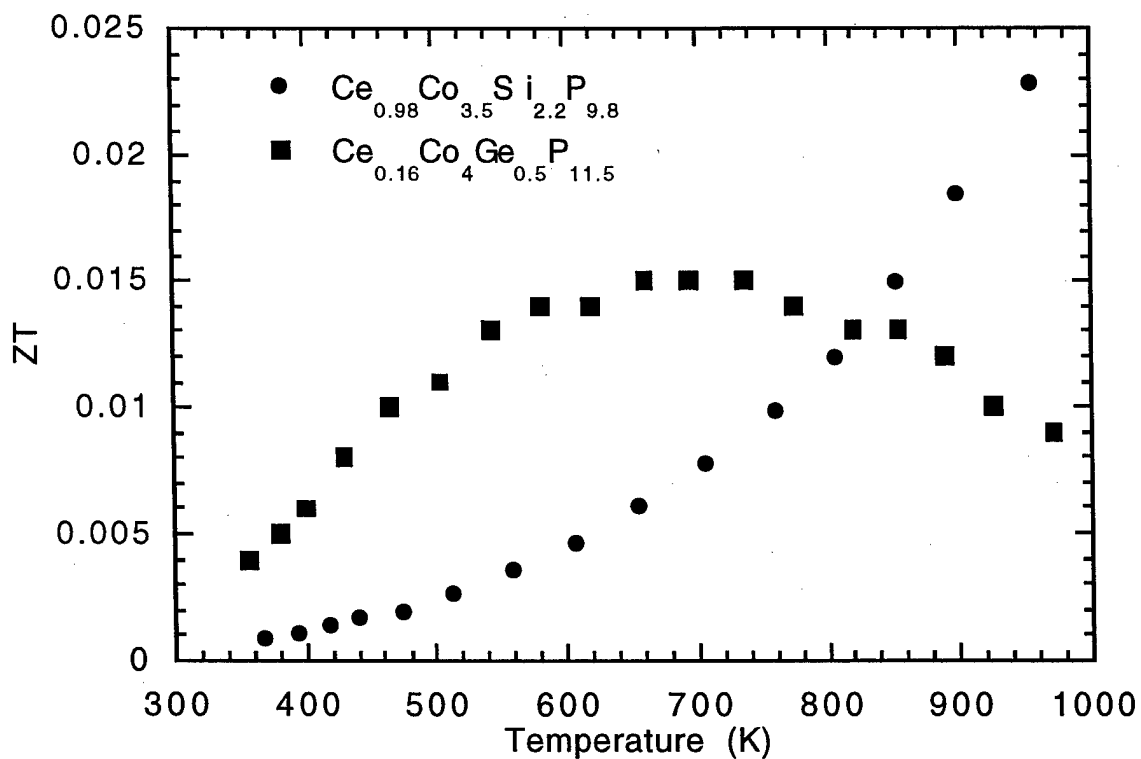Figure 25. Thermal conductivity as a function of temperature

Figure 26. ZT as a function of temperature

49

E. Comparison of the Thermoelectric Properties of CoP_3 and $CeFe_4P_{12}$ Synthesized by Two Techniques

It is important to discuss the effect impurities may play on the properties of some phosphide skutterudites, especially those prepared by the flux technique. Although Sn impurities have not been detected in the skutterudite phases using electron microprobe analysis, it may be present at levels detectable only by other more sensitive techniques. The effect of Sn impurities on skutterudite properties is not known at these concentration levels. To determine whether Sn impurities affect properties, we prepared two skutterudites by both the direct synthesis (DS) and Sn flux techniques.

Figure 27 shows the electrical resistivity of CoP_3 and $CeFe_4P_{12}$, each synthesized by two different techniques. Both CoP_3 samples had resistivity values that were almost identical. For $CeFe_4P_{12}$, however, the resistivity values were similar above 540 K but started deviating significantly as the temperature decreases below this temperature. It is possible that this is the extrinsic region where impurities dominate the conduction behavior. Lower temperature measurements for both samples are necessary to determine whether that is the case. The Seebeck coefficient is plotted in Figure 28. The values and trend agree well in the case of $CeFe_4P_{12}$. The values for CoP_3 (DS) are slightly larger than those of CoP_3 (Flux) which corresponds to a slightly higher electrical resistivity in the former sample.

Figure 29 shows that the thermal conductivity of $CeFe_4P_{12}$ prepared by the two techniques are not much different. A big difference is, however, obvious in CoP_3 samples and this is mainly due to a relatively large difference in their densities. Nevertheless, when the effects of sample density on thermal conductivity are corrected, ZT values are calculated for all four compounds. The values seem to agree very well within experimental errors and it also seems that the ZT values can be used as an index to determine the transport properties of these compounds.
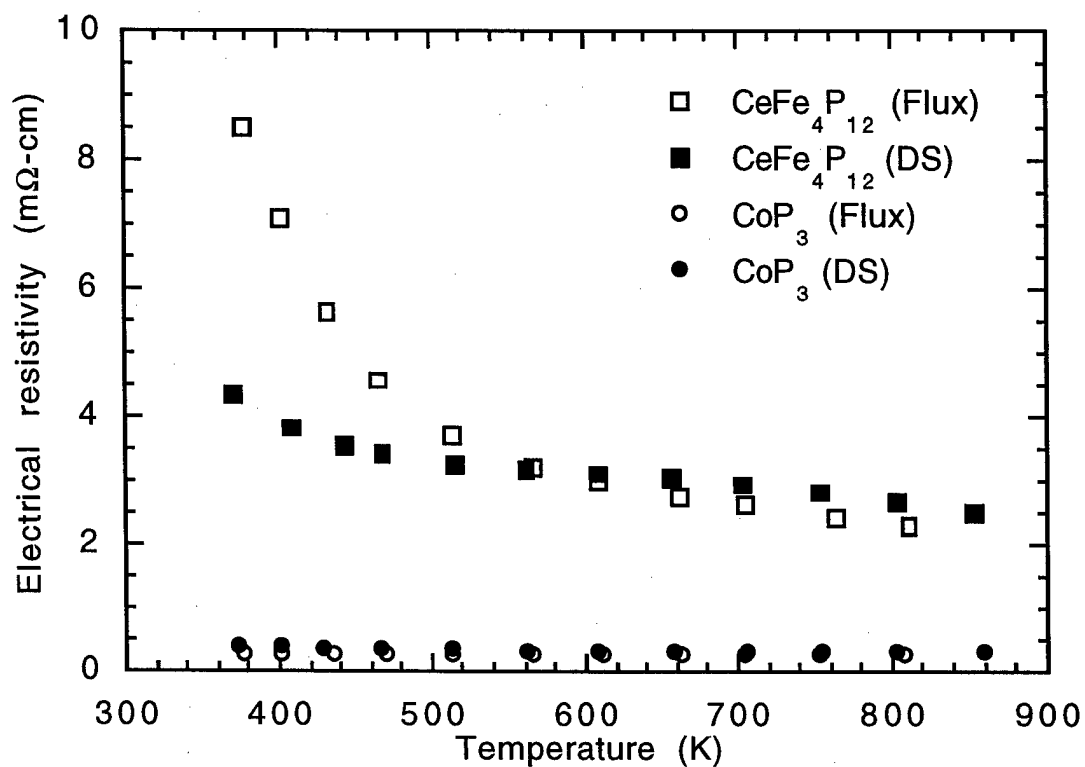
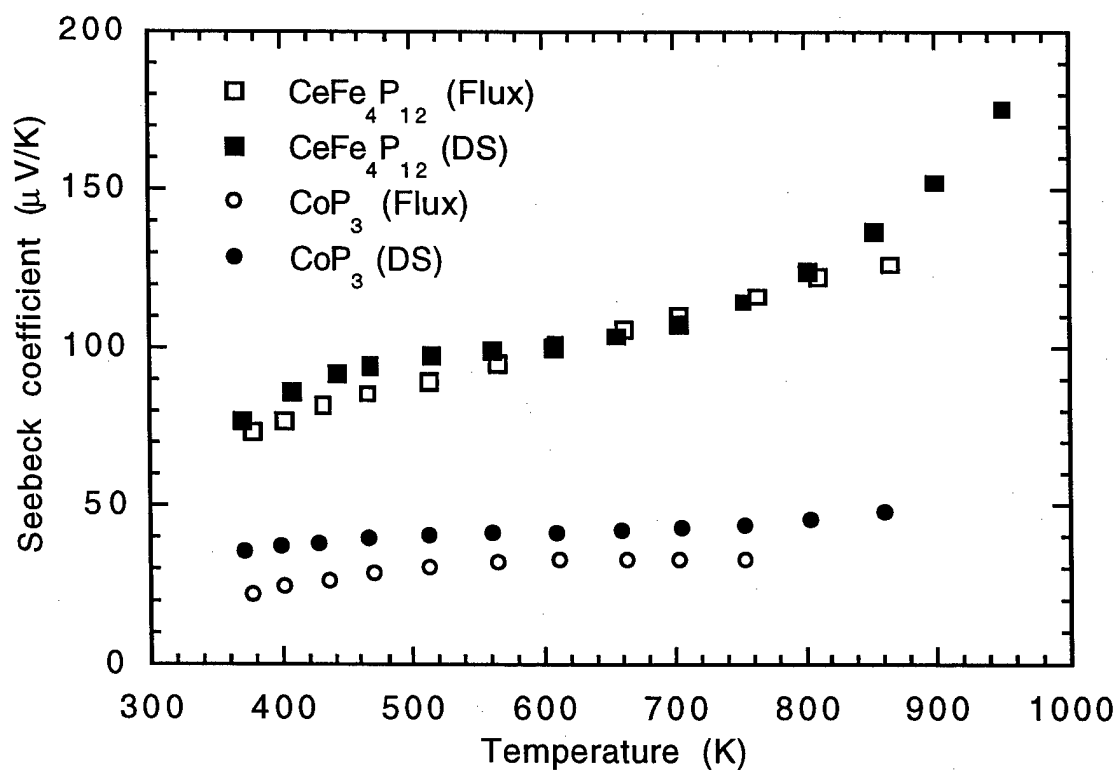Figure 27. Electrical resistivity as a function of temperature

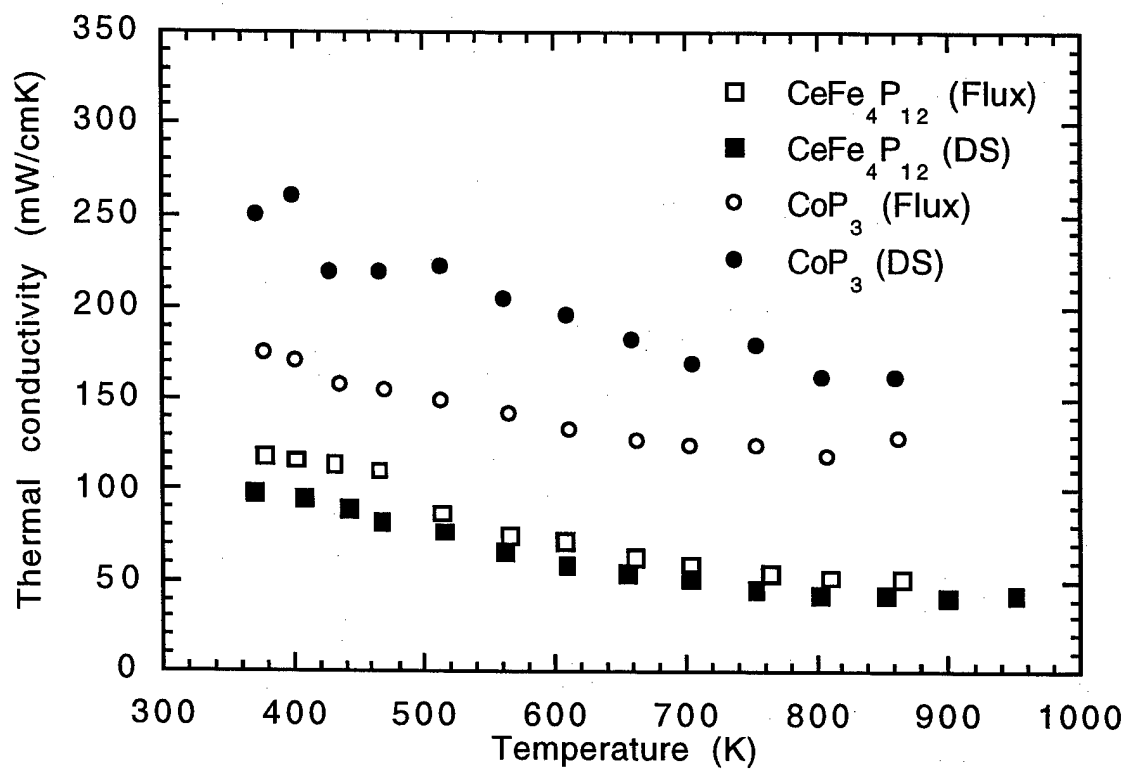Figure. 28. Seebeck coefficient as a function of temperature

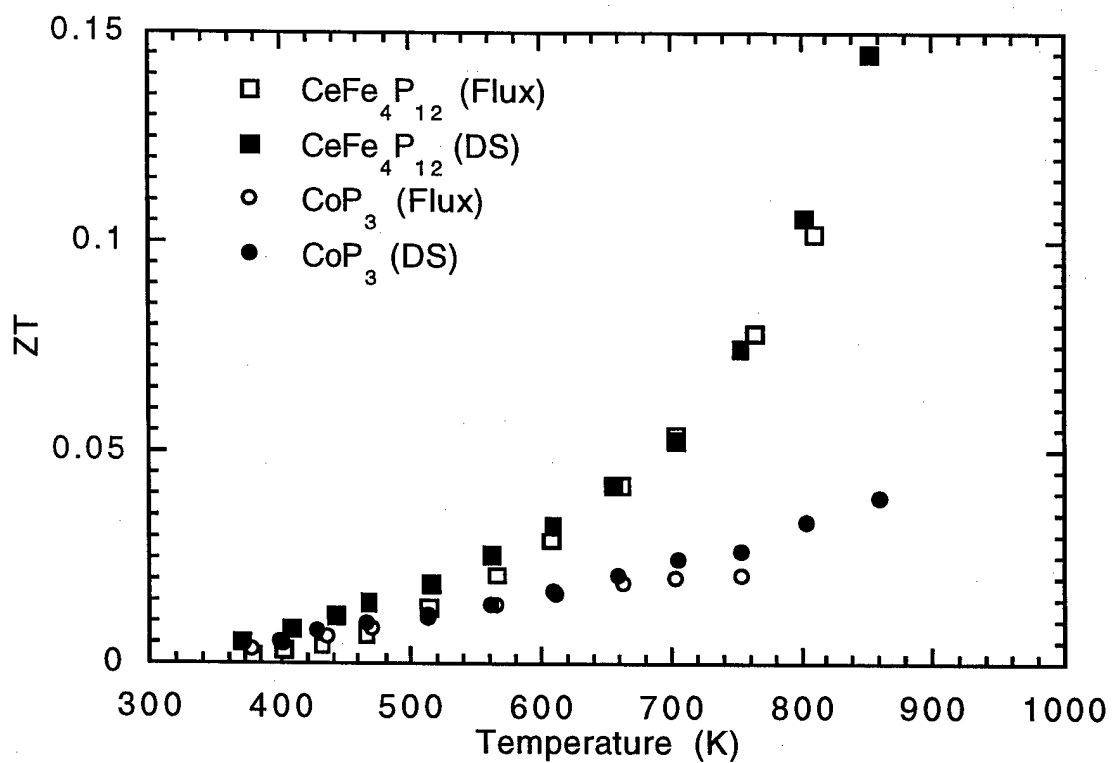Figure 29. Thermal conductivity as a function of temperature

Figure 30. ZT as a function of temperature

F. Comparison Between Phosphide and Antimonide Skutterudites

Room temperature properties of a binary phosphide and two filled ternary phosphide skutterudites as well as their antimonide analogs are listed in Table 11. From this table, it is quite surprising that $CeFe_4Sb_{12}$ would give the best thermoelectric properties considering its high carrier concentration. From our study of the phosphides, the best material in this class in $CeFe_4P_{12}$, which suggest that the combination of Ce and Fe in the skutterudite structure may be the reason for these good thermoelectric properties. The property that may have some correlation between the $CeFe_4Sb_{12}$ and $CeFe_4P_{12}$ is the Seebeck coefficient (Fig. 32), where both of them have the same trend as well as similar magnitude as the temperature increases.

Table 11. Room temperature properties of some phosphide and antimonide skutterudites

	Units	CoP_3	$CoSb_3$	$CeRu_4P_{12}$	$CeRu_4Sb_{12}$	$CeFe_4P_{12}$	$CeFe_4Sb_{12}$
Lattice constant	(Å)	7.7073	9.0345	8.0419	9.2657	7.7917	9.1350
Percentage of theoretical density	%	87	99.9	87.1	97	99	99
Type of conductivity		p	p	p	p	p	p
Electrical resistivity	$m\Omega cm$	0.26	0.44	14	0.31	20.5	0.75
Seebeck coefficient	$\mu V/K$	15	108	137	31	58	59
Hall carrier concentration	$10^{19}/cm^3$	3.26	1	7.2	207	1.42	550
Hall mobility	cm^2/Vs	748	1432	7.8	10	24.9	1.5
Thermal conductivity	mW/cmK	185	100	86*	40	140	14

*extrapolated value

In Figure 31, the electrical resistivity of the phosphides and antimonides are plot as a function of temperature. The behavior of these compounds seem to follow the trend that the compounds that form from larger anions will tend to be more metallic like. The interesting aspects of the phosphides and antimonides skutterudites lie in their difference in thermal conductivity. Figure 33 shows these differences. It is well known that compounds containing heavier atoms tend

to possess the lower lattice thermal conductivity and this seems to be the case for $CoSb_3$ whose thermal conductivity is about two times less than that of CoP_3. In the ternary compounds, $CeFe_4Sb_{12}$ has a thermal conductivity about ten times lower than that of $CeFe_4P_{12}$ at room temperature, but the difference becomes smaller as the temperature increases. This seems to be mainly due to additional lattice scattering by Ce atoms rattling in the voids of skutterudite structure. The cage size (and lattice constant) relative to the size of filling atoms are thus important in order to effectively scatter phonons. For the case of $CeRu_4P_{12}$, its lattice constant is slightly larger than that of $CeFe_4P_{12}$ and it does have lower thermal conductivity below 660 K. For $CeRu_4Sb_{12}$, however, it becomes even more metallic than that of $CeFe_4Sb_{12}$ and the large part of its thermal conductivity comes from electronic contribution.

Figure 34 compares the ZT values of the phosphides and antimonides in this study. Although all of the antimonides have larger ZT values than the phosphides, from our studies, it has been shown that it should be possible to improve the properties of the phosphide compounds by at least two to three times their current ZT values by producing n-type filled ternary compounds and/or forming arsenide solid solutions.
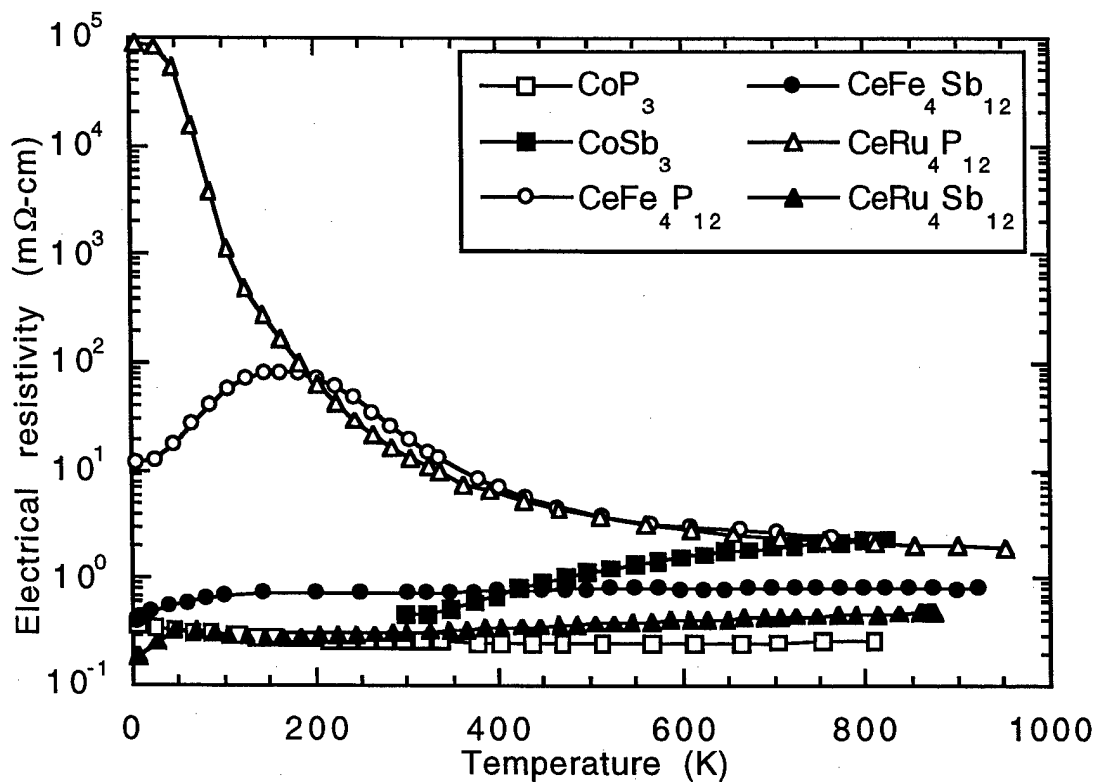
Figure 31. Electrical resistivity as a function of temperature (Antimonide data are from JPL.)
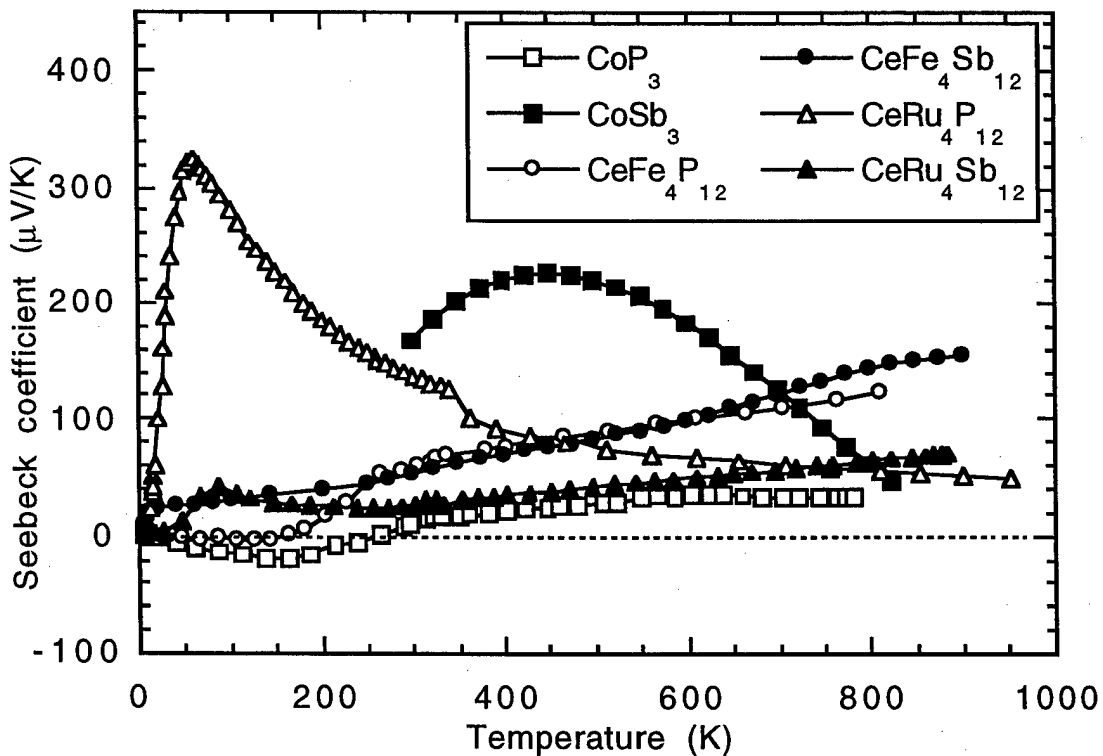

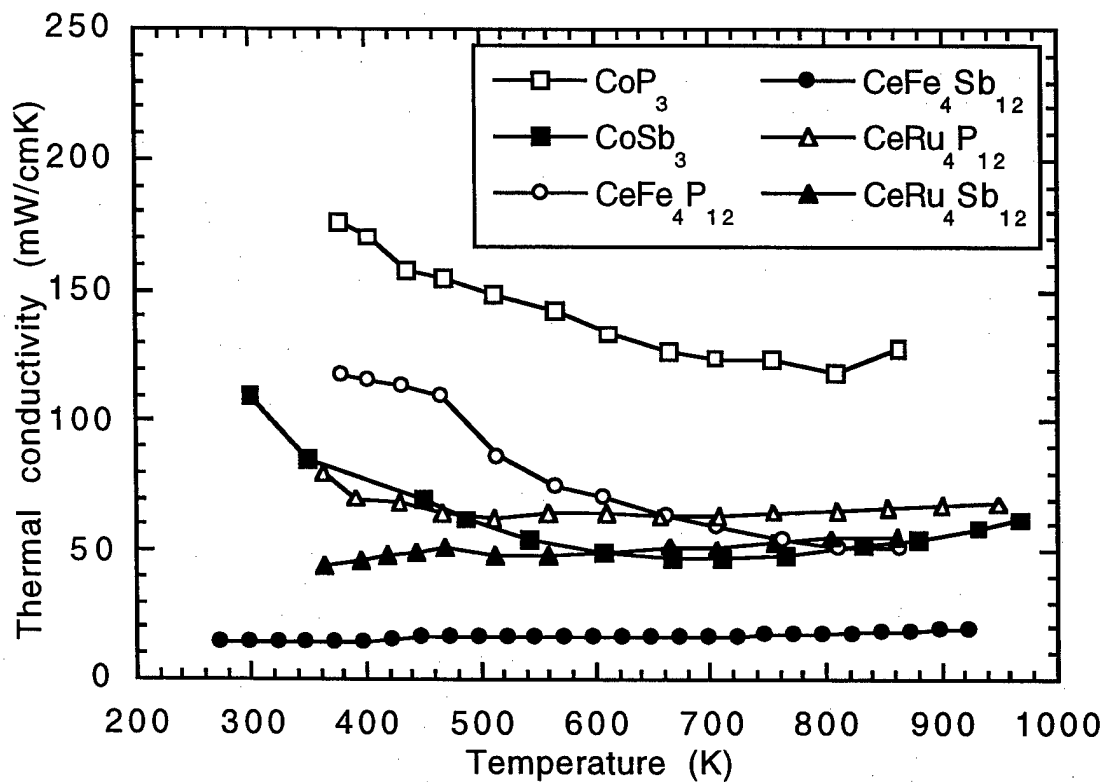Figure 32. Seebeck coefficient as a function of temperature (Antimonide data are from JPL.)

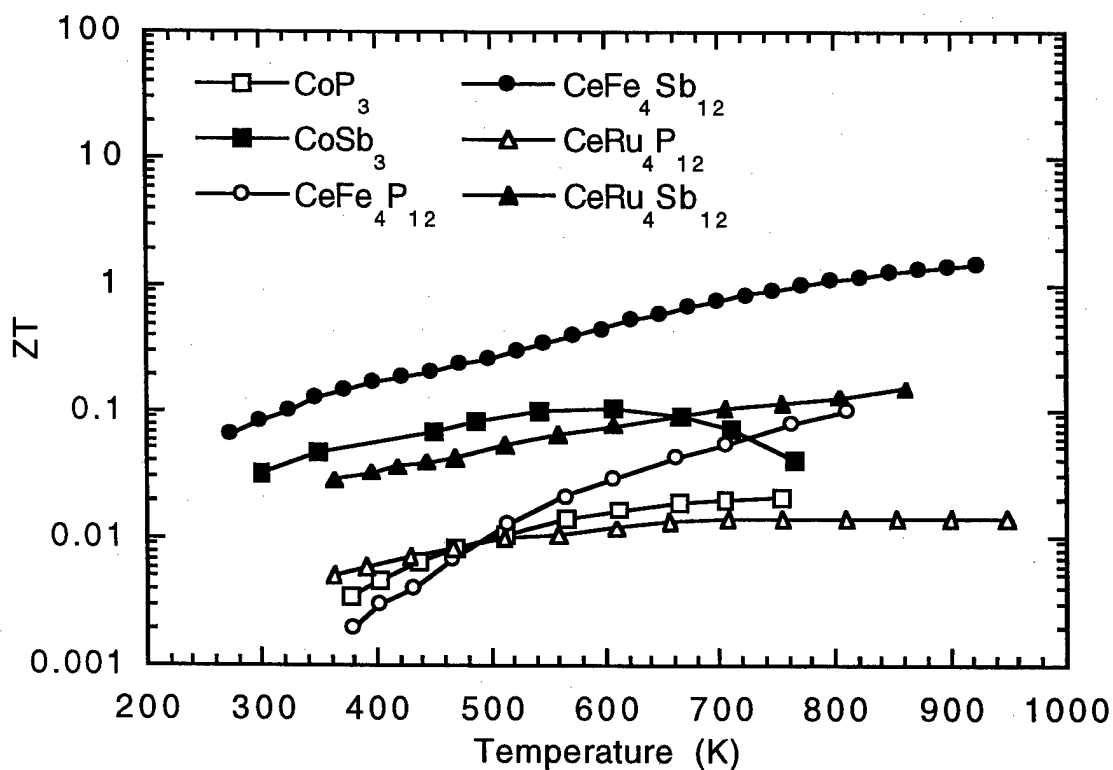Figure 33. Thermal conductivity as a function of temperature. (Antimonide data are from JPL.)

Figure 34. ZT as a function of temperature

V. Conclusions

During the course of this program, a number of phosphide based skutterudite materials were synthesized and their transport properties studied. A number of experimental techniques were used for the preparation of these compounds, despite some challenging problems related to the synthesis of materials containing phosphorus. Electrochemical synthesis was shown for the first time to be a viable technique to make powder or thin films of the skutterudites although experimental conditions still need to be optimized. Some important findings related to the chemistry and thermodynamic of the phases formed during synthesis using these three techniques were discussed and the information extracted was used successfully in preparation of these materials.

The thermoelectric data measured on the phosphide-based skutterudites has provided important new information on the transport properties of this class of compounds. They vary with doping, solid solution, ion size and mass, etc. Some of the synthesized materials exhibit semiconducting behavior, in agreement with previous theoretical and experimental findings. Although most of the phosphides studied exhibited p-type conduction, n-type materials could be prepared by doping with some atoms such as the rare-earth elements. Not only does this doping affect the electrical properties, it also causes a reduction in the lattice thermal conductivity due to extra phonon scattering by these dopants.

The results from the study of $CoP_{3-x}As_x$ solid solutions showed an unexpected enhancement in the Seebeck coefficient and figure of merit. This approach when applied to the ternary skutterudites for examples, $CeFe_4P_{12-x}As_x$, $CeFe_{4-x}Co_xP_{12-x}As_x$, etc. may lead to significantly improved ZT values. Comparison between phosphide and antimonide skutterudites has provided experimental proof that there is a change in electrical properties from semiconducting to semimetallic/metallic behavior as well as an increase in carrier effective mass when smaller atom such as P are replaced by larger sized atom such as Sb. We believe that by continuing to study the phosphide, arsenide and antimonide skutterudites and their solid solutions, we will gain the

knowledge to improve the thermoelectric properties in this class of compounds beyond their current limitations.

VI. REFERENCES

1. T.J. Seebeck, 'Magnetische Polarisation der Metalle und Erze durch Temperatur-Differnz', *Abhandlungen der Deutschen Akademie der Wissenschaften zu Berlin*, 265-373 (1822)

2. J.C. Peltier, 'Nouvelles expériences sur la caloricité des courans electriques', *Annales de chimie*, **LVI**, 371-87 (1834)

3. W. Thomson, 'On a mechanical theory of thermoelectric currents', *Proceedings of the Royal Socity of Edinburgh*, 91-8 (1851)

4. B. Sherman, R. Heikes, and R. Ure, *J. Appl. Phys.*, **31**, 1 (1960)

5. R.R. Heikes and R.W. Ure, *Thermoelectricity: Science and Engineering*, Interscience Publishers, NY (1961)

6. D.M. Rowe and C.M. Bhandari, *Modern Thermoelectrics*, Reston Publishing Company, Inc., VA, (1983)

7. A.F. Ioffe, see *Doklady Akademie nauk SSSR*, **106**, 981 (1956)

8. A.F. Ioffe, '*Semiconductor Thermoelements and Thermoelectric Cooling*', Inforsearch, London, (1957)

9. T. Caillat, J.-P. Fleurial and A. Borshchevsky, *Proc. XV Int. Conf. Thermoelectrics*, Pasadena, California, March 26-29 (1996)

10. T. Caillat, J.-P. Flueurial, *Proc. 31st Intersoc. Ener. Conv. Engin. Conf.*, Washington, D.c., August 11-16, pp. 905-909 (1996)

11. J.-P. Fleurial, A. Borshchevsky, T. Caillat, D.T. Morelli an dG. P. Meisner, *Proc. XV Int. Convf. Thermoelectrics*, Pasadena, California, March 26-29 (1996)

12. I. Oftedal, *Z. Kristallogr. A* **66**, 517 (1928)

13. J.-P. Fleurial, T. Caillat, and A. Borshchevsky, *Proc. XIV Intl. Conf. Thermoelectrics*, St. Petersburg, Russia, June 27-30, 231 (1995)

14. T. Caillat, J.-P. Fleurial and A. Borshchevsky, to be published in Proc. XV Int. Conf. Thermoelectrics, Pasadena, California, March 26-29 (1996)

15. C. Sales, D. Mandrus, and R.K. Williams, *Science* **272**, 1325 (1996)

16. D. Jung, M.H. Whangbo, S. Alvarez, *Inorganic Chemistry* **29**, 2252 (1990)

17. F. Grandjean, A. Gèrard, D.J. Braun, W. Jeitschko, *J. Phys. Chem. Solids* **45**, 8/9, 877 (1984)

18. N.T. Stetson, S.M. Kauzlarich, H. Hope, *J. Solid State Chem.* **91**, 140 (1991)

19. W. Jeitschko and D. Braun, *Acta Cryst. B* **33**, 3401 (1977)

20. L. Nordstrom and D. Singh, *Phys. Rev. B* **53**, 3, 1103 (1996)

21. I. Shirotani, T. Adachi, K. Tachi, S. Todo, K. Nozawa, T. Yagi and M. Kinishita, *J. Phys. Chem. Solids* **57**, 2, 211 (1996)

22. G.A. Slack, *New Materials and Performance Limits for Thermoelectric Cooling*, CRC Handbook of Thermoelectrics, Ed. M. Rowe, CRC Press, pp. 407-440 (1995)

23. J.P. Odile, S. Soled, C.A. Castro & A. Wold, *Inorg. Chem.* **17**, 2, 283 (1978)

24. G. Kliche, *Solid State Commun.* **80**, 1, 73 (1991)

25. W. Biltz and M. Heimbrecht, *Z. Anorg. Allgem. Chem.* **241**, 349 (1939)

26. S. Rundqvist and E. Larsson, *Acta Chem. Scand.* **13**, 551 (1959)

27. S. Rundqvist and N.-O. Ersson, Ark. Kemi, 30, 103 (1968)

28. F.-E. Faller, E.F. Strotzer and W. Biltz, *Z. Anorg. Allgem. Chem.* **244**, 317 (1940)

29. S. Rundqvist, *Nature* **185**, 31 (1960)

30. F. Hulliger, *Helv. Phys. Acta* **34**, 782 (1961)

31. C.E. Myers, *High Temp. Science* **6**, 309 (1974)

32. P. Joibois, *C. R. Acad. Sci. (Paris)* **150**, 106 (1910)

33. K. Zeppenfeld and W. Jeitschko, *J. Phys. Chem. Solids* **54**, 11, 1527 (1993)

34. W. Jeitschko and R. Rühl, *Inorg. Chem.* **21**, 1886 (1982)

35. G.P. Meisner, Ph.D. Thesis, University of California, San Diego (1982)

36. R.P. Guertin, C. Rossel, M.S. Torikachvili, M.W. McElfresh, and M.B. Maple, S.H. Bloom, Y.S. Yao, M.V. Kuric and G.P. Meisner, *Phys. Rev. B* **36**, 16, 8665 (1987)

37. G.P. Meisner, *Physica B* **108**, 763 (1981)

38. L.E. DeLong and G.P. Meisner, *Solid State Commun.* **53**, 2, 119 (1985)

39. D.J. Braun and W. Jeitschko, *J. Less-Common Met.* **76**, 33 (1980)

40. S. Zemni, D. Tranqui, P. Chaudouet, R. Madar, J.P. Senateur, *J. Solid State Chem.* **65**, 1 (1986)

41. J. Ackermann and A. Wold, *J. Phys. Chem. Solids* **38**, 1013 (1977)

42. R.A. Munson and J.S. Kasper, *Inorg. Chem.* **7**, 390 (1968)

43. I. Shirotani, E. Takahashi, N. Mukai, K. Nozawa, M. Kinoshita, T. Yagi, k. Suzuki, T. Enoki and S. Hino, *Jpn. J. Appl. Phys.* **32**, Suppl. 32-3, 294 (1993)

44. C. Sekine, H. Saito, T. Uchiumi, A. Sakai and I. Shirotani, *Solid State Commun.* **106**, 7, 441 (1998)

45. D.T. Morelli, G.P. Meisner, B. Chen, S. Hu and C. Uher, *Phys. Rev.* B **56**, 12, 7376 (1997)

46. B. Chen, J.-H. Xu, C. Uher, D.T. Morelli, G.P. Meisner, J.-P. Fleurial, T. Caillat and A. Borshchevsky, *Phys. Rev. B* **55**, 3, 1476 (1997)

47. P.M. Chene, *Ann. de Chim.* **15**, 187 (1941)

48. J.J. Cuomo and R.J. Gambino, *J. Electrochem. Soc.* **115**, 755 (1968)

49. R.C. DeMattei, D. Elwell and R.S. Feigelson, *J. Crystal Growth* **44**, 545 (1978)

50. R.C. DeMattei, D. Elwell and R.S. Feigelson, *J. Crystal Growth* **43**, 643 (1978)

51. R.S. Feigelson, *Solid State Chemistry: A Contemporary Overview* , Advances in Chemistry Series, 186, ed. by S.L. Holt, J.B. Milstein and M. Robbins (American Chemical Society, Washington, D.C., 1980), p. 243 - 275

52. K. Ishida and T. Nishizawa, *Binary Alloy Phase Diagrams*, 270 (1990)

53. K. Ishida and T. Nishizawa, *Binary Alloy Phase Diagrams*, 1234 (1990)

54. K. Ishida and T. Nishizawa, *Binary Alloy Phase Diagrams*, 1219 (1990)

55. P.C. Donohue, *Mat. Res. Bull.* **7**, 9, 943 (1972)

56. McCormack and J. -P. Fleurial, *Modern Perspectives on Thermoelectrics and Related Materials*, MRS Symp. Proc. 234 (Materials Research Society, Pittsburgh, Pennsylvania), p. 135 (1991)

57. C. Wood, D. Zoltan and G. Stapfer, *Rev. Sci. Instrum.* **56**, 5, 719 (1985)

58. W. Vandersande, C. Wood C., A. Zoltan and D. Whittenberger D., *Thermal Conductivity* , Plenum Press, New York, 445 (1988)

59. C. Maxwell, *Treatise on electricity and magnetism Vol.I*, Oxford University Press, London, p.365 (1873)

60. W.R. Rayleigh, *Phil. Mag.,* **5**, (1892) 481

61. A. Watcharapasorn, R.C. DeMattei, R.S. Feigelson, T. Caillat, A. Borchevsky, G.J. Snyder, and J.-P. Fleurial, J. Appl. Phys. **86**, 11, 6123 (1999)

62. M. Fornari and D.J. Singh, *Phys. Rev. B,* **59**, 15, 9722 (1999)

63. M. Llunell, P. Alemany, S. Alvarez, V.P. Zhukov and A. Vernes, *Phys. Rev. B,* **53**, 16, 10605 (1996)

64. D.T. Morelli, G.P. Meisner, B. Chen, S. Hu and C. Uher, *Phys. Rev. B,* **56**, 12, 7376 (1997)

65. H.D. Lutz and G. Kliche, *J. Solid State Chem.* **40**, 64 (1981)

66. M.S. Abrahams, R. Braunstein and F.D. Rosi, *J. Phys. Chem. Solids* **10**, 204 (1959)

67. F.D. Rosi, *Soid State Electronics* **11**, 833 (1968)

68. A.J. Cornish, *J. Electrochem. Soc.* **106**, 685 (1959)

69. H.D. Lutz and G. Kliche, *Z. Anorg. Allg. Chem.* **480**, 105 (1981)

VII-A. Publications and Presentations

1. A. Watcharapasorn, R.C. DeMattei, R.S. Feigelson, T. Caillat, A. Borshchevsky, G.J. Snyder, and J.-P. Fleurial, J. Appl. Phys. **86**, 11, 6123 (1999)

2. A. Watcharapasorn, R.C. DeMattei, R.S. Feigelson, T. Caillat, A. Borchevsky, G.J. Snyder, and J.-P. Fleurial, *Mat. Res. Soc. Symp. Proc.* **626** (2000)

3. A. Watcharapasorn, R.C. DeMattei, R.S. Feigelson, T. Caillat, A. Borchevsky, G.J. Snyder, and J.-P. Fleurial, *Proceedings of the 18th International Conference on Thermoelectrics* (Baltimore, MD, 1999), p. 462

4. A. Watcharapasorn, R.C. DeMattei, R.S. Feigelson, T. Caillat, A. Borchevsky, G.J. Snyder, and J.-P. Fleurial, Poster Presentation at the 17th Conference on Crystal Growth and Epitaxy (AACG/West), Fallen Leaf Lake, California (June 4-7, 2000)

5. A. Watcharapasorn, R.C. DeMattei, R.S. Feigelson, T. Caillat, A. Borchevsky, G.J. Snyder, and J.-P. Fleurial, Poster Presentation at the 11th American Conference on Crystal Growth & Epitaxy (ACCGE-11) and Short Course on Crystal Growth & Epitaxy, Tuczon, Arizona (July 31 - August 6, 1999)

VII-B. Program Participants

A. FACULTY AND STAFF	POSITION
R.S. Feigelson	Director, Advanced Materials Processing Lab Professor (Research), Materials & Engineering Department
R.C. DeMattei	Senior Research Associate

B. GRADUATE STUDENT	DEPARTMENT
A. Watcharapasorn	MS&E

C. OTHER ASSOCIATES	INSTITUTION
J.-P. Fleurial	Jet Propulsion Laboratory
T. Caillat	Jet Propulsion Laboratory
A. Borshchevsky	Jet Propulsion Laboratory
G.J. Snyder	Jet Propulsion Laboratory
D.J. Singh	Naval Research Laboratory
M.D. Carelli	Westinghouse Electric Corporation
D.V. Paramonov	Westinghouse Electric Corporation
G.A. Slack	Rensselaer Polytechnic Institute